Alma Mater Studiorum - Università di Bologna

DOTTORATO DI RICERCA IN

SCIENZE CHIRURGICHE

Ciclo 35

Settore Concorsuale: 06/D4 - MALATTIE CUTANEE, MALATTIE INFETTIVE E MALATTIE DELL'APPARATO DIGERENTE

Settore Scientifico Disciplinare: MED/35 - MALATTIE CUTANEE E VENEREE

DERMOSCOPIC, HISTOPATHOLOGIC AND MOLECULAR CHARACTERIZATION OF HEAD AND NECK MELANOMA

Presentata da: Martina Lambertini

Coordinatore Dottorato

Bianca Maria Piraccini

Supervisore

Emi Dika

Esame finale anno 2023

ABSTRACT

Almost 18-35% of cutaneous melanomas are located in the head and neck region (2-5% of them in the scalp) and according to multiple epidemiological studies they are supposed to have a worse prognosis with respect to those of other body areas.

The aim of this phD project is to perform a global evaluation of head/neck region cutaneous melanomas with a distinct analysis of histological, dermoscopic and molecular features of the selected cases. The objective is to help clinicians and surgeons in the diagnosis and management of the lesions in this peculiar body area. Finally, the molecular analysis aims to investigate potential markers that can provide further insights for the diagnosis and treatment of melanomas with specific adverse prognostic features.

The diffuse distribution of folliculotropism (≥3 HF/specimen), the presence of atypical melanocytes into the isthmus, and the perifollicular involvement were associated with melanoma recurrence. The dermoscopic parameter *grey circles* in lentigo maligna was correlated to the depth of folliculotropism, with a higher probability of an isthmic or bulge follicular extension of neoplastic melanocytes. The detection of *grey circles, light/dark brown pseudonetwork* and *light brown structureless areas* in lentigo maligna melanoma was associated with the distribution of folliculotropism (focal/diffuse).

MiR-146a-5p expression was shown to be significantly greater in melanomas with a mitotic rate ≥1/mm2 as well as in ulcerated lesions compared to those without ulceration. No difference emerged evaluating regression when considering all melanomas subtypes, but an higher expression was noticed in the lentigo maligna melanoma group. Moreover, miR-146a-5p expression was lower in head/neck region cutaneous melanomas with Breslow thickness ≥0.8 mm.

These results give further insights for the management of cutaneous melanomas with specific adverse prognostic elements. As the majority of head/neck region cutaneous melanomas are wild type of *BRAF* and *NRAS* mutations and not suitable for targeted therapies, the discovery of new molecular targets may provide relevant opportunities for their treatment.

INTRODUCTION

The incidence of cutaneous melanoma (CM) has increased in the past decades, accounting for up to 5% of all skin tumors, but determining up to 65% of the deaths.[1–3] Established risk factors include phenotypic features (fair phototypes, high nevi count, positive family history), ultraviolet radiation exposure (natural and artificial) and genetic mutations.[1] Up to 15% of CMs arise in subjects of the same family. Germline mutations in the high-penetrance CM susceptibility gene *CDKN2A* (*cyclin-dependent kinase inhibitor 2A*) have been detected in 5-40% of patients with familiar CMs and in 8-15% with sporadic multiple CMs.[1,4–6] Other susceptibility genes include *MITF, CDK4, POT1, ACD, TERF2IP, BAP1* and *TERT*.[1]

HEAD AND NECK MELANOMA

The head and neck region (HNR) accounts for only 9% of the total body surface, but almost 18-35% of global CMs are located in this area and more frequently in those parts with chronic actinic damage (cheeks, neck, scalp, nose and outer portion of the ear); 2-5% of them in the scalp (fig. 1).[7–13] According to multiple epidemiological studies, HNR CMs, especially scalp lesions, are supposed to have a worse prognosis with respect to those of other body area.[7,11,12,14–16] Indeed, the scalp and the facial/nose area have a different density of hair follicles (HFs) and a diverse exposition to environmental factors, even if they belong to the same HNR.[14] A large cohort study reported a 5-year and 10-year Kaplan-Meier survival probability for HNR CMs subjects of 83.1% and 76.2%, respectively, compared to 92.1% and 88.7%, respectively, for CMs at other body areas.[17] De Giorgi et al. in 2012 reported a significantly lower 5-year overall survival probability for HNR CMs compared to other cutaneous sites (78.9 versus 93.1%; p=0.05) as well as a further lower rate for face/neck CMs compared to scalp lesions (81.8% vs 66.7%)[14]. Lachiewicz et al. showed that neck and scalp CMs accounted for 6% of total cases, but were associated to 10% of all deaths and were

associated to a two times greater rate of CM-specific death compared to those lesions of the extremities, after controlling for age, sex, Breslow thickness, and ulceration.[17] In 1985, Benmeir et al. defined scalp CM as the "invisible killer".[18] Recently, Elshot et al. reported that LM/LMM were not an independent prognostic factor in predicting the outcome of HNR CMs, but LM/LMM subtype was related to specific clinicopathological features, including anatomic area in a cosmetic and functional sensitive area, elderly age, and a low positive yield of sentinel lymph node biopsy (SLNB).[19] The reasons are not completely clear and possible explanations include: a) a specific CM biological behavior and a greater development of lesions with a rapid vertical growth (nodular and desmoplastic CMs), b) delayed diagnosis due to hair coverage or anatomical limits, c) greater cumulative sun exposure, d) anatomical aspects, including the rich vascular supply and the complex lymphatic system representing an obstacle to the SLNB and therefore the subsequent possibility to the prompt start of adjuvant therapies.[7,13,16] Sentinel lymph nodes in the periparotid/intraparotid areas are hard to biopsy because of the strict connection with the facial nerve, while the location of the CM close to the cervical lymphatics is associated to the difficulty to discriminate the radioactive signal of the sentinel node from the primary injection site.[11]

Fig. 1. A lentigo maligna melanoma on the bald scalp of a patient with chronic actinic damage.

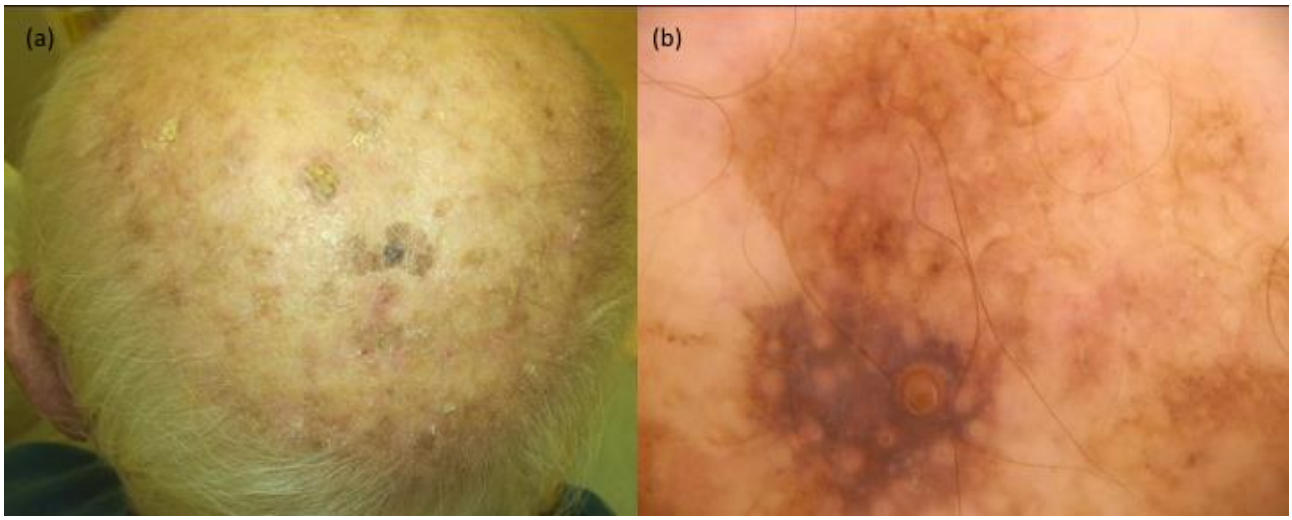

Ultraviolet (UV) radiations contribute to CM pathogenesis, especially in older patients with bald/hair thinning scalp with chronic photodamage and solar keratoses; genetic factors seem to be more relevant in younger subjects.[7,12,20] A paper published in 2019 reported a lower survival associated to CMs of the posterior scalp, that is less exposed to UV radiations also in subjects with androgenetic alopecia: those lesions had worse histopathological features (higher rates of satellite metastasis, increased mitoses), being more frequently nodular.[21]

In the last few years, there has been a focus in the literature on the role of follicular involvement by neoplastic cells in melanomagenesis, but there is not an univocal interpretation.[7]

HNR CMs are likely associated to two scenarios: a) LM/LMM subgroup on bald/hair thinning scalps and skin with chronic actinic damage of older subjects that are more often diagnosed earlier due to the easier detection and maybe the slow growth (fig. 1), and b) a different subgroup of CMs on hairy scalp in younger people with a later and more invasive diagnosis (fig. 2).[16]

Fig. 2. A nodular melanoma on the hairy scalp of a patient.

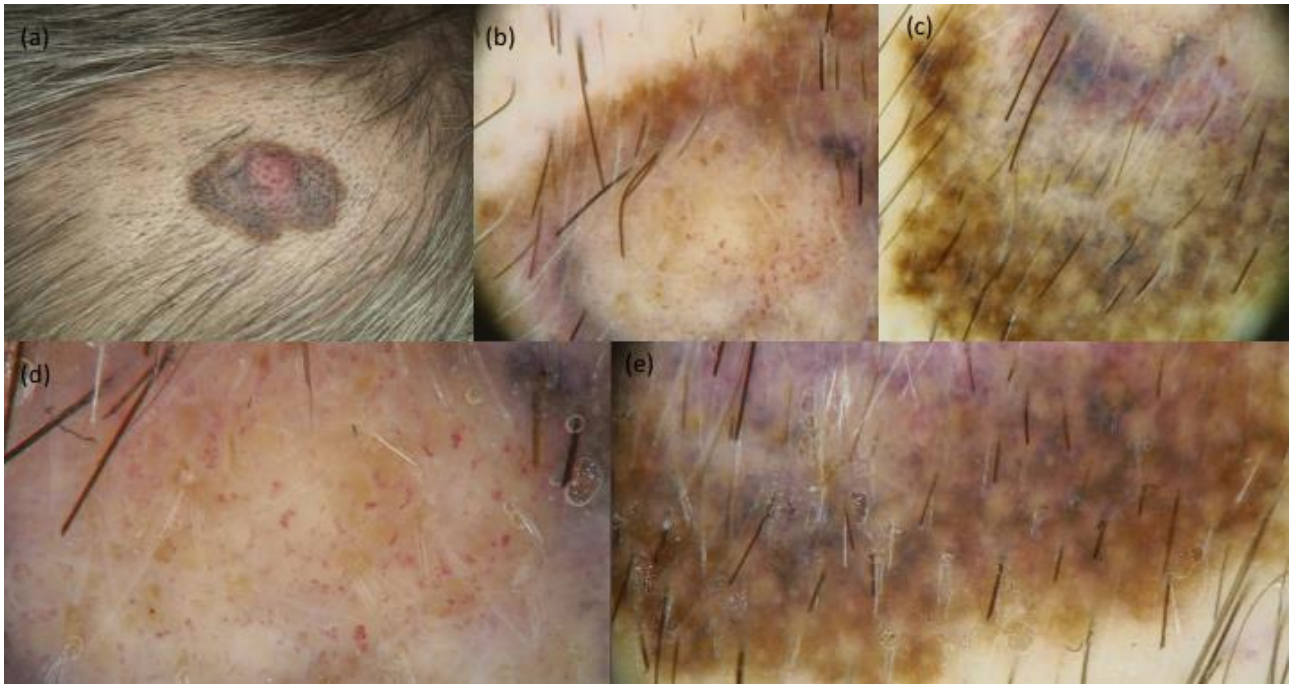

HNR CMs seem to have a different pathogenetic mechanism compared to CMs of other body areas. Different theories have been proposed, including 1) a theory of site-dependent susceptibility of melanocytes to neoplastic degeneration and 2) a different response to the mitogenic stimulus of UV radiations according to anatomic area.[22,23] A "*divergent pathways model*" of CMs with two main categories has been proposed: 1) the "nevogenic", related to melanocyte proliferation proneness and 2) the other with cumulative solar damage.[24] Both pathways have an initial step with the activation of melanocytes based on the UV exposure in the early life and host factors; then the evolution to CM depends on exogenous and endogenous factors. Nevogenic CMs develop in subjects constitutively prone to melanocytic proliferation, with a high nevi count and low actinic damage, more often in young/middle-aged patients in body areas with an intermittent sun-exposure (i.e. trunk) (fig. 3a). On the contrary, CMs of the second group arise mostly in older patients with a low number of nevi on chronically sun-exposed skin, with solar elastosis, such as the HNR (fig. 1 e 3b).

Fig. 3. A subject constitutively prone to melanocytic proliferation, with a high nevi count and a low actinic damage (a); a patient with a low number of nevi on a chronically sun-exposed skin with chronic actinic damage and multiple solar lentigos (b).

The main histopathological subtypes of HNR CMs include: superficial spreading CMs (25-46% of invasive cases), lentigo maligna and lentigo maligna melanoma (21-49% of invasive cases), nodular CMs (20-29%) and, rarely, desmoplastic CMs.[25,26]

A report of 2017 showed that CMs on bald/thinning hair scalp had a greater Breslow thickness than those on hairy scalp; on the opposite side, subjects with CM on fully covered scalp had thinner neoplasms and were younger.[12] This trend was inverted in the report by Pereira et. al. who showed that CMs arising on hairy scalp were more often invasive (81%) with a greater median Breslow thickness (0.8±1.3 mm) compared to those of exposed scalps (43%; 0±0.6 mm), p=0.004.[16] Nevertheless, the Authors specified that Breslow thickness and mitotic rate were not statistically different in the two groups when evaluating exclusively the invasive cases (n=55). Recently, Bracaccio et al. suggested that scalp CMs might have a greater Clark level compared to non-scalp lesions independently from Breslow thickness, due to the thinner dermis in this area compared to other regions. The higher probability of a subcutaneous spreading (Clark V level) in scalp CMs may be associated to the great density of HFs enhancing the neoplastic diffusion to subcutaneous fat.[27]

In a number of cases, varying between 5.3 and 10% in the reported studies, scalp CMs are firstly observed by hairdressers that have a greater chance to explore the skin covered by hair compared to the patients themselves.[20,28] A study in 2013 analyzed data from self-administered questionnaires hand-delivered to certified hairdressers at 45 hair salons in California: 91.7% wanted to discover more information about CM and 93.5% was interest in informing clients after a specific training.[29] However, the role of medical screening is preeminent and CMs diagnosed by physicians seem to have a lower Breslow thickness compared to those observed by the patient or other subjects, underlying the necessity of a full body examination.[7,16] Thus, the scalp inspection is not always routinely performed by dermatologists, but this practice should be highly encouraged.

Dermoscopy of CM can reveal a multicomponent pattern with an atypical pigmented network, irregular streaks or a bluish veil.[7] Dermoscopy of LM/LMM of chronically photo-damaged areas

shows *asymmetrically pigmented follicles*, *circles within the circles*, *rhomboidal structures*, *obliterations of the hair follicles*; the presence of shades of *grey* can favor the diagnosis.[7]

Surgery is still the gold standard for the treatment of CM, but a number of nonsurgical treatments, including radiotherapy and topical therapies (i.e. imiquimod), are applied, considering the mean older age of patients and the subclinical extension of the neoplastic cells.

Local recurrence rate of HNR CMs range between 2.8% and 28% and rates of positive margins after conventional surgery are up to 21% in the upper portion of the face.[30] The reported local recurrence rates for LM treated with different margin-controlled surgical procedures, including Mohs micrographic surgery and slow Mohs, are up to 12% and the time to recurrence are reported to be quite long and heterogeneous, ranging between 1 month and 8 years.[31] The risk of progression of LM to LMM has been estimated to be around 5%.[32] The long time to local recurrence has relevant implications in the long term clinical management of LM patients. Radical excision is sometimes hard to be obtained in the HNR, due to the possibility to obtain wide surgical margins in those areas with high esthetic and functional impact and to the microscopic tumor extension beyond the visible margin, named "subclinical extension" (fig. 4).[30] Shin et al. showed that significant risk factors for subclinical spread of invasive CM include anatomic location on the HNR, previous treatments, age >65 years, and the presence of mitoses.[30]

Fig. 4. A patient with a wide lentigo maligna melanoma of the forehead, before (a) and after (b) the surgical excision and the need of a skin graft.

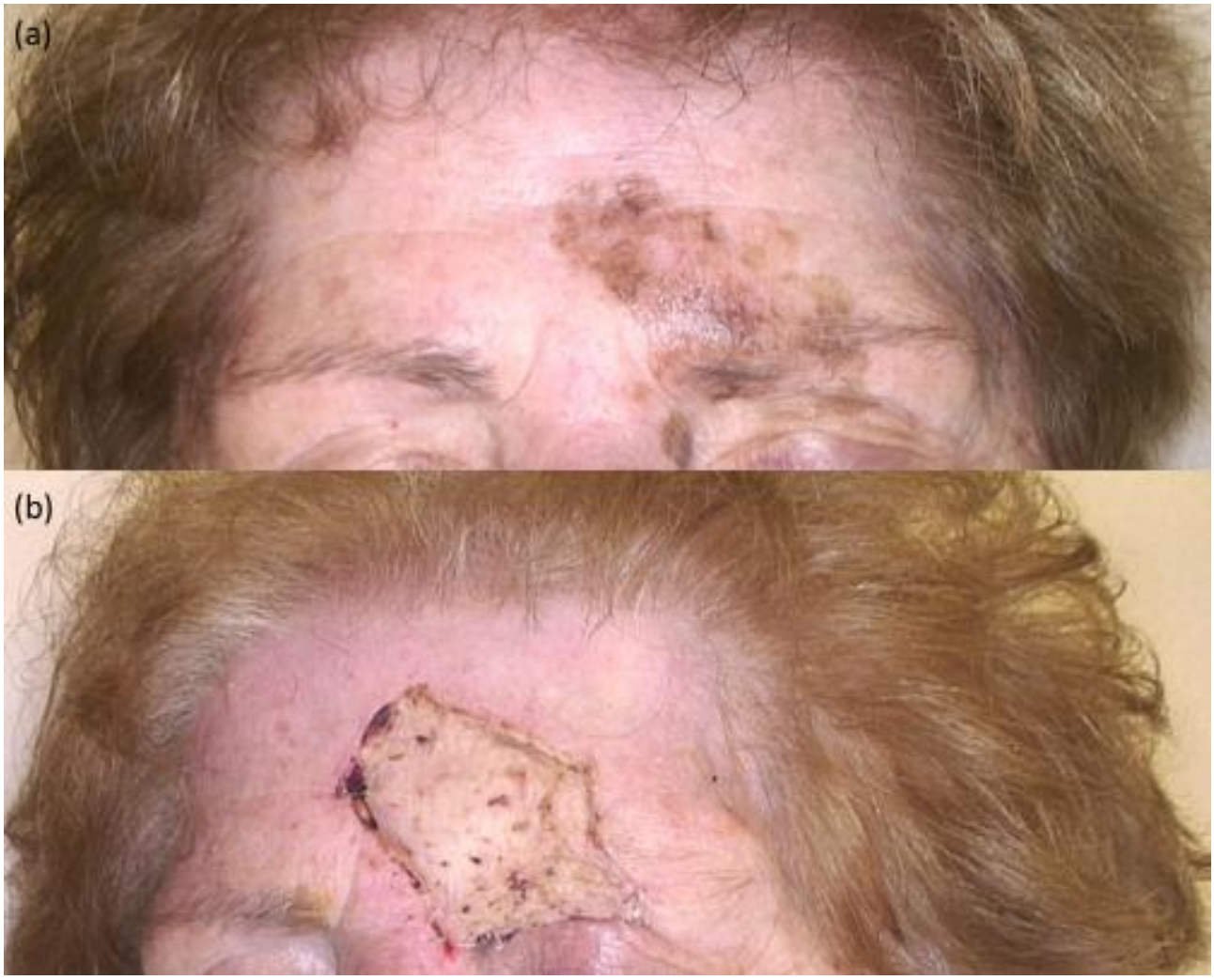

Regarding the use of topical imiquimod, three recent systematic reviews on the treatment of LM reported similar histological clearance rates of almost 76%; a number of >60 applications (OR >7.8) or a frequency of >5 applications per week (OR >6) were reported to be related to a higher probability of histologic clearance.[33] Guitera et al. proposed three subgroups of patients potentially suitable for imiquimod treatment: 1) presence of multiple comorbidities, older patients or previous multiple recurrences, 2) subjects with multiple consecutive histologic positive margins, 3) younger subjects with cosmetic issues that want to avoid potential 'disfiguring' procedures. In group 3 a close follow-

up is mandatory to assess recurrences or disease progression and surgical procedures are required in case of imiquimod failure.[33]

FOLLICULOTROPISM AND MELANOMA

Cutaneous surface is supposed to be constituted by five millions HFs.[34] The HF likely interacts with the neuroendocrine system having a role in the immune-surveillance against pathogens. The stem cells in the hair bulge have been extensively investigated and they can be classified in in three main groups: epithelial, melanocytic and mesenchymal cells.[35] Epithelial stem cells express cytokeratins, adhesion molecules, cytokines and growth factor receptors and have a key contribution in the hair cycle regeneration.[36–40] The outer root sheath includes melanocytic stem cells that are precursors of differentiated melanocytes.[41–43] Mesenchymal stem cells are supposed to have hematopoietic properties.[44] Neural crest-like multipotent stem cells express embryonic stem cell markers that are precursors of many lineages.[45]

The spreading of atypical melanocytes to the HF is named "*folliculotropism*" (fig. 5) and it has been categorized into three different groups: "*primary follicular melanoma*" (FMM), "*melanoma with folliculotropism*" (MMF) and "*invasive melanoma arising from melanoma in situ*" (MISF). FMM primarily involves the HF with secondary extension of atypical melanocytes to the epidermis, MMF occurs on the epidermis with the extension of atypical melanocytes to the HF, and MISF is an in-situ CM but with the invasion of the HF. Folliculotropism involving the infundibulum is a not uncommon in CM and specifically in LMM, but lentiginous diffusion of melanocytes into HF has also been observed in a subgroup of benign nevi or in melanocytic hyperplasia on sun-damaged skin.[26,27,28] The prognostic significance of folliculotropism has been not totally elucidated and reported data in the current literature are not unilateral: some Authors support the role of HF as a physical and immunologic barrier to the neoplastic spreading, but it has even been reported that the phenomenon may play a role in CM melanoma progression.

Fig. 5. Spreading of atypical melanocytes to the hair follicle (folliculotropism), H&E: (a) ×4 and (b) ×10.

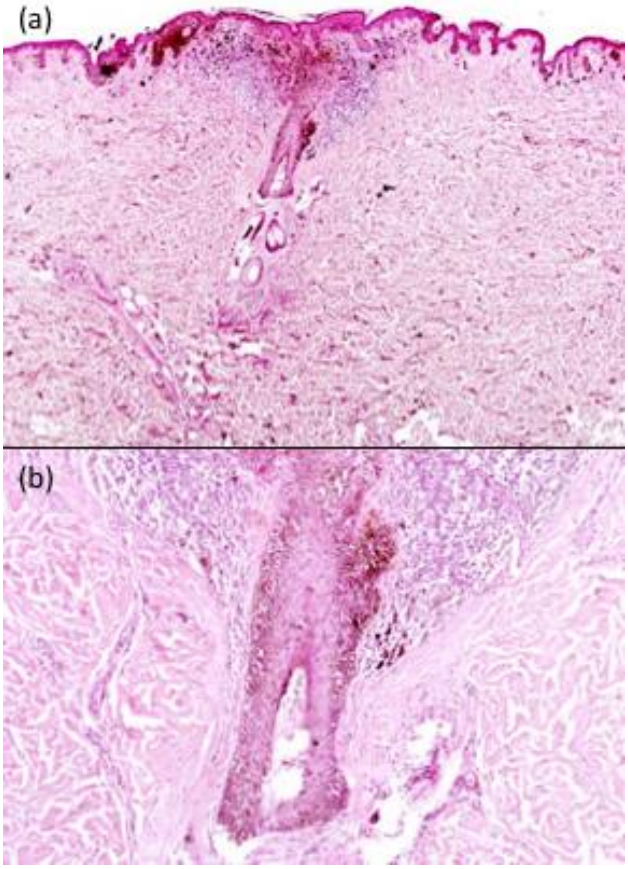

Perifollicular and follicular destructive invasion by atypical melanocytes was reported to be a potential contributing element to CM metastases development in 5/8 specimens of thin, low-risk CMs with no potential histological parameters with a risk of progression (vertical growth, ulceration, regression or abundant mitoses).[46] Further investigations were reported in 2004 by Hantschke et al., describing FMM with neoplastic cells primarily invading the HF, but some with secondary localization within the epidermis.[47] In the reported cases, contrary to LMM, the depth of follicular involvement appeared to be deeper than the length of interfollicular epidermal involvement: these lesions arose mainly in the skin of older patients with chronic photo damage. On the contrary, Pozdnyakova et al. considered the HF a physiological barrier and an obstacle of the intraepithelial spread of neoplastic melanocytes beyond the level of the stem cell niche in the bulge.[48] One-hundred

specimens of CM were evaluated (61 in situ and 39 invasive CM with relevant in situ components) and 82 samples with folliculotropism: 57/82 showed the presence of atypical melanocytes within the infundibulum 24/82 in the isthmus. The neoplastic involvement of bulge was observed exclusively in 1 case. This phenomenon was supposed to be based on the finding that the human bulge outer root cells overexpress CD200R, a type 1 transmembrane glycoprotein that provides a negative feed-back through the interplay with CD200R on the myeloid lineage cells and CD4þ and CDT cells.[48–50] Furthermore, unknown cell mediators supposedly expressed in the deeper portion of the HF might block the neoplastic spreading: tenascin-C, a glycoprotein implicated in the epithelial-microenvironment interaction during the process of tumor progression, was proposed.[48,51] It has also been proposed that peptide fragments of hair lysates may provide natural protection against cancer, inhibiting the proliferation of CM cells in vitro.[7,52]

The assessment of folliculotropism was recommended in the histopathological diagnosis of CM in 2013 by the *International Collaboration on Cancer Reporting* (ICCR), but this practice is not regularly applied.[53] Tjarks et al. in 2017 suggested to assess the 'follicular Breslow depth', from the granular cell layer to the deepest atypical melanocyte extending from the follicular epithelium, in order to decide the proper clinical and surgical management and follow-up.[54] Nevertheless, this parameter may overrate the risk of disease progression and is not correct to omit the conventional Breslow thickness.[54,55]

MicroRNAs AND MELANOMA

In the last twenty years the altered expression of small ncRNAs, including microRNAs (miRNAs) and long noncoding RNAs (lncRNAs) has been extensively investigated in cancer. The ENCODE project showed that 80% of the human genome is biochemically functional and non-coding transcripts represent the majority of RNA molecules generated from the active genome, accounting for up to

97% of the transcriptome.[56,57] MicroRNAs (miRNAs) represent a group of small non-coding RNAs that are usually 22–25 nucleotides in length. The function of miRNAs alteration in CM development has been shown in multiple studies, with both oncogenic and oncosuppressive properties.[58] Oncogenic miRNAs (oncomiRs) target and downregulate tumor suppressor genes, while specific miRNAs play a suppressive function in downregulating genes related to neoplastic proliferation and spreading.[59] The imbalance of these subgroups of miRNAs has a key role in melanomagenesis.

MiR-211-5p exhibits the greatest variance in CM with respect to normal melanocytes.[60–62] MiR-211-5p is transcribed by *MITF* together with its host gene, *melastatin* (*TRPM1*), in human melanocytes. In CM neoplastic process, TRPM1/miR-211 are frequently under-expressed or lost.[63] MiR-21-5p, miR-135a and miR-155 play a role in CM proliferation with an up-regulation in neoplastic cells compared to benign melanocytic lesions, and metastases.[64–66] Let-7 family is essential in the regulation of cellular proliferation and let-7a, let-7b and let-7d are under-expressed in benign nevi compared to CM.[67]

A number of miRNAs are known to be under-expressed in CM, including miR-125b, miR-126/126*, miR-136, miR-145, miR-194, miR-203, miR-205, miR-206, miR-365, and miR-485-5p.[68–72]

On the contrary, an over-expression of miR-15b and miR-4286 has been detected, with a role in increasing proliferation and preventing apoptosis.[73]

MiR-125b can influence programmed death cell processes: indeed, miR-125b transfected cells exhibit higher values of *p27*, *p53* and *p21*, and subsequent induced senescence.[74] Mir-205 is known to induce apoptosis and its under-expression in metastatic CMs may induce the activation of *E2F transcription factor 1* (*E2F1*) and the inhibition of *retinoblastoma protein* (*Rb*).[75] Mir-26a has been reported to be downregulated in neoplastic cells with respect to healthy and its replacement favors apoptosis through the *anti-apoptotic protein silencer of death domains* (SODD).[76]

The role of miRNAs in CM metastatic processes has been extensively evaluated. MiR-150 was reported to be over-expressed in CM and metastases with respect to normal nevi, likely related to the ability to target *v-myb avian mieloblastosos viral oncogene homolog* (MYB), *early growth response*

2 (EGR2), neurogenic locus notch homolog protein 3 (NOTCH3) and immune system-related genes, cytokine signaling cascade and G-protein.[77–81] MiR-211 over-expression seems to be associated to a lower CM invasiveness through the reduced expression of *transforming growth factor beta* (*TGFB*), *brain-specific homeobox/POU domain protein* (*BRN2*) and *ion channel KCNMA1*.[61,62,82] MiR-200 family is over-expressed in melanoma cells increasing tumoral spreading: miR-200c induces an amoeboid–like invasion pattern, downregulating *MARCKS*, as well as a protrusion-associated elongated migration related to a lower actomyosin contractility.[83] MiR-182 resulted over-expressed in CM favoring the development of distant metastases due to the silencing of *FOXO3* and *MITF*.[84–86]

Specific miRNAs are down-regulated in the metastatic process: miR-34a, miR-203, miR-124, miR-125b, miR-137, 153-3p, miR-542-3p, miR-625 and miR-9. MiR-9 is associated to the lower regulation of *zinc finger protein SNAI1* and *nuclear factor kappa-light-chain-enhancer of activated B cells* (*NF-κB1*) and the upregulation of *E-cadherin***.**[87–92]. MiR-7-5p is a strong inhibitor in the development of distal metastases, partly due to the silencing of *RelA/NF-κB* signaling.[93]

The role of miRNAs dysregulation has been even described even in multiple primary CMs compared to single CMs, as the prognosis of MPMs patients is a matter of debate.[94,95] In 2021, Dika et al. published the first global molecular characterization of MPMs with the analysis of miRNome with a small RNA-seq approach, showing a peculiar expression pattern of MPM with respect to isolated CM. MPMs miRNome resulted more similar to benign nevi, favoring the hypothesis of a less aggressive behavior: globally, 22 miRNAs resulted differentially expressed in MPMs with respect to single CMs. Moreover, the Authors reported that isomiR-125a-5p was tenfold over-represented in CM than the canonical form and differentially expressed in MPMs of the same patient.[96]

Variations in miRNA length and sequence are a known occurrence, but the biological meaning of miRNA variants or isoforms (isomiRs) is not fully understood. IsomiRs could derive from alternative Drosha and or Dicer cleavage of the precursor miRNAs or from post-transcriptional changes made by *nucleotidyl transferase*, incorporating nucleotides to the pre-miRNA or mature miRNA ends.[97,98]

In 2021, Broseghini et al. reported that that 55 mature miRNAs were differentially expressed between early-stage CM and benign nevi and specifically they showed 18 canonical miRNAs and 37 isomiRs.[3] IsomiRs may result more expressed compared to the canonical miRNA or they may manifest a different modulation in normal or neoplastic cells. In their paper, the majority of the isomiRs had the same expression variation than the canonical miRNA, but they describe a number of exceptions with an inverse trend.[3] MiR-30d-5p and miR-30a-5p had isomiRs with reverse trends: miR-30a-5p|0|+2 and miR-30d-5p|0|+2 were over-expressed in early-stage CMs, while miR-30a-5p|0|−1, miR-30a-5p|0|−2 and miR-30d-5p|0|−1 resulted downregulated compared to benign nevi specimens.

The alteration of specific miRNAs has been even related to traditional histopathological features, including Breslow thickness. Dika et al. in 2020 reported that miR-21-5p and miR-146a-5p expression was significantly related with Breslow thickness in SSM, but not in NM, and that their assessment in biopsy specimens might be helpful to support standard Breslow thickness evaluation.[59] The aim of the Authors was to investigate the potential use of miRNAs as prognostic adjuvant biomarkers in CM, taking into account that Breslow thickness is considered the most relevant parameter for CM staging and an independent prognostic factor. Nevertheless, a study evaluating the interobserver variability in the histologic parameters of CM revealed a discordance rate of 87% in any variable, with a subsequent variation in clinical *American Joint Committee on Cancer* stage in 17%, as well as a 65.8% rate of discordance in Breslow thickness assessment.[99]

The aim of this phD project is to perform a global evaluation of HNR CM with a distinct analysis of histological, dermoscopic and molecular evaluations of the selected cases. The objective is to help clinicians and surgeons in the diagnosis and management of CMs in this peculiar body area. The definitive surgical management of HNR CMs is often a multistage process because of the frequent occurrence of similarly appearing lesions that require incisional biopsy prior to final radical excision.[11] Moreover, the differential diagnosis of pigmented lesions on body areas with chronic

cumulative actinic damage is challenging. Surgeons sometimes have to face with wide pigmented lesions in sensitive areas and a pre-operative diagnosis of the whole lesion may be difficult (fig. 4a). Indeed, a wide ‘solar lentigo like lesion’ may contain heterogeneous areas of LM or solar lentigo/atypical solar lentigo and atypical melanocytic hyperplasia (fig. 4a). LMM is identified in 5 to 52% of LM specimens after total excision. It is hard to assess isolated atypical cells or distinguish them from melanocytic hyperplasia in area chronically photo-exposed.[33]

Finally, the molecular analysis aims to investigate potential markers that can provide further insights for the diagnosis and treatment of CM with specific adverse prognostic features.

THE PROJECT

HISTOPATHOLOGICAL ANALYSIS: THE ROLE OF FOLLICULOTROPISM

Materials and methods

We retrospectively analyzed consecutive cases of primary HNR CMs excised and evaluated from January 2005 to December 2016 at the Melanoma Unit and Laboratory of Histopathology, Dermatology, IRCCS Azienda Ospedaliero-Universitaria di Bologna, University of Bologna (study protocol authorized by the local ethics committee - Nr. DERM-MTC 2017).

All specimens had been obtained from deep excisional biopsies or wide excisions, with a width of 0.5 to 2 cm. The hematoxylin and eosin slides were reviewed independently by two dermatopathologists (C.M. and B.C.), who evaluated the presence of folliculotropism. The amount of HFs in every single sample ranged from 4 to 6, so we analyzed a median of 3 units. The presence of atypical melanocytes in the HFs was recorded according to the following categories: (1) absent—no involvement, (2) focal—involvement (<3 HF/specimen) and (3) diffuse—involvement (≥3 HF/specimen, and (4) not evaluable (fig. 6 and 7). We classified the folliculotropism into the following categories: (1) infundibulum, (2) isthmus, (3) bulb, or (4) not evaluable. The perifollicular extension in the adjacent dermis was recorded and classified as (1) absent or (2) present.

The follicular Breslow thickness, calculated from the top of the epidermal granular layer to the deepest atypical melanocyte in/around the follicular structure, was re-assessed and compared to the conventional Breslow thickness. Other evaluated histologic parameters were: histopathologic subtype of CM, ulceration, mitotic rate/mm^2, lymphovascular invasion, tumor-infiltrating lymphocytes, solar elastosis, and satellite metastases. Patients' data were evaluated, including sex, age at diagnosis, and the anatomic site [(1) scalp, (2) face (including forehead, nose, and cheeks), and (3) neck]. Mucosal

and ocular melanomas were excluded. Data regarding the survival were evaluated, such as the cause of death and presence of recurrences.

Fig. 6 Facial superficial spreading melanoma with Breslow thickness of 1 mm and diffuse proliferation of atypical melanocytes in nest and solitary units in the infundibulum and isthmus of all follicles, H&E: (a) ×4 and (b) ×10.

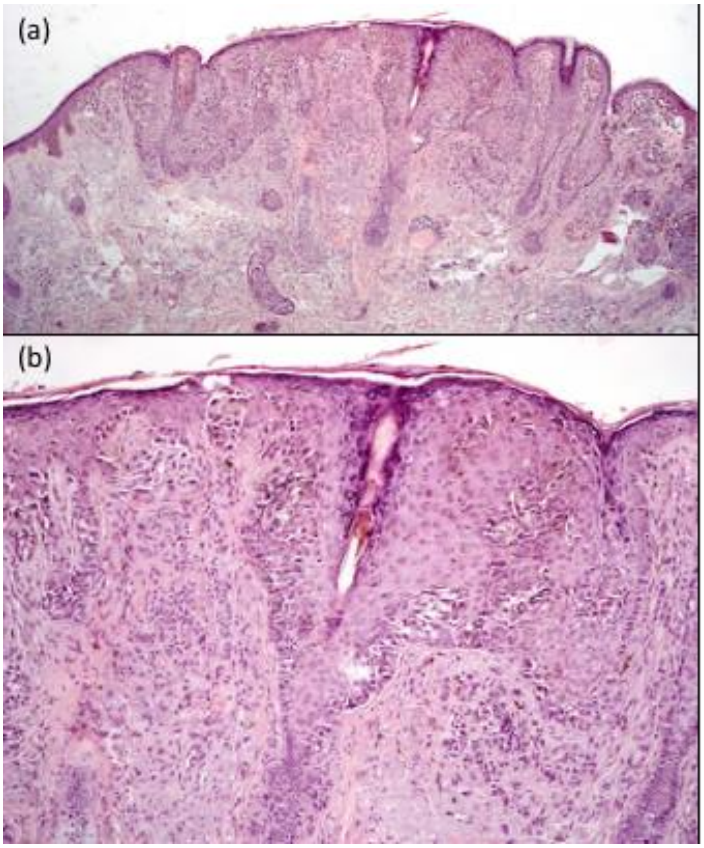

Fig. 7. Facial nodular melanoma with Breslow thickness of 3.2 mm and diffuse proliferation of atypical melanocytes in nest and solitary units in the infundibulum and isthmus of follicles, H&E (a) ×2 and (b) ×4.

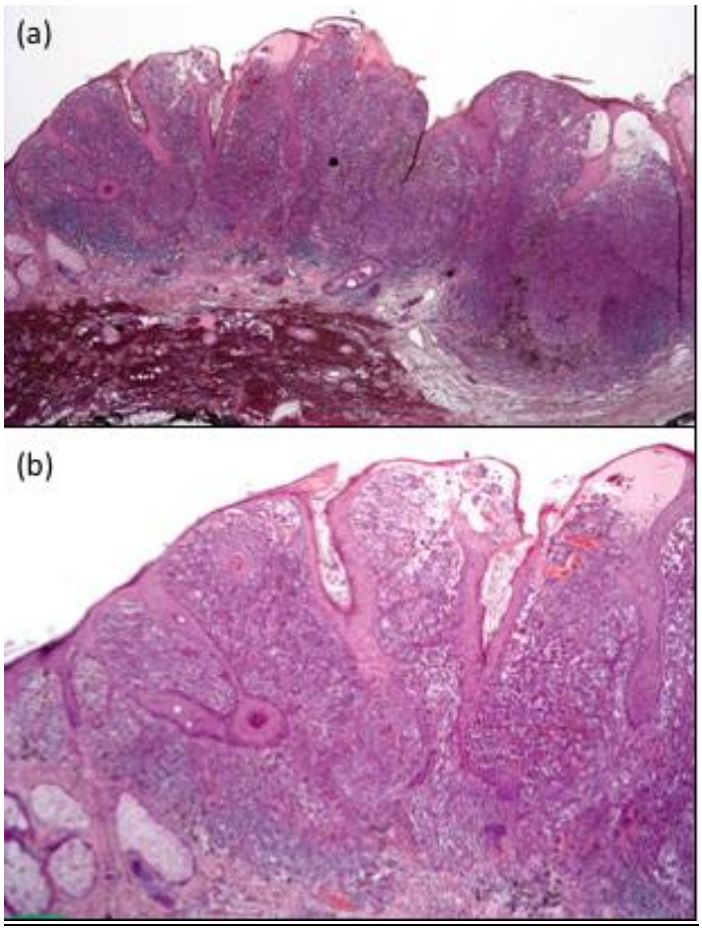

Statistical Analysis

In the bivariate statistical analysis, the Pearson $\chi 2$ test was employed to test for independence when categorical variables were compared. The only continuous variables were the age and Breslow thickness. For the former, t test could be used because all the assumptions were satisfied, whereas the Kruskall-Wallis test was used for the thickness because the normality assumptions were rejected by the Shapiro-Wilk test.

Results

Globally, 62 patients with CMs (24 women and 38 men) were analyzed, with an age ranging from 25 to 91 years. Males had a lower mean age at the diagnosis compared to females (average age 66.08 years vs 71.79 years). The face was the most common area, followed by the scalp and the neck. The Breslow thickness varied from 0.2 to 8 mm. Globally, 22 cases of LMM (35.5%), 27 cases of SSM (43.5%), and 13 cases of NM (21.0%) were recorded (tables 1, 2, 3). All samples were diagnosed as CMs with folliculotropism (melanoma arising in the epidermis with involvement of follicular units) and no cases of primary follicular CMs were noticed. Diffuse and focal folliculotropism were observed in 28 and 27 specimens, respectively. The other 7 samples were NM with destroyed follicles (n = 3), SSM without evidence of HF involvement (n = 2), and LMM without folliculotropism (n = 2). SSMs and LMMs showed a similar follicular involvement. NMs manifested a greater tendency to diffuse folliculotropism. Diffuse and focal subtypes were equally located in the face and neck, but the diffuse subtype was more frequent in the scalp. The presence of folliculotropism was related to a greater Breslow thickness (P<.001).

The extension of neoplastic melanocytes into the isthmus was detected in 31 samples (50.0%) and into the infundibulum in 18 cases (29.0%), but into the bulb only in 2 cases (3.2%) of LMM. In 11 NM (17.8%) a total destruction of the HF by CM cell and tumor inflammatory infiltrate was observed. Two cases did not display follicular involvement. The perifollicular extension in the adjacent dermis was noticed in 23 cases. Cohen κ was used to determine if there was agreement between Breslow thickness and follicular Breslow thickness. There was a moderate agreement between the two parameters ($\kappa = 0.604$, $P < .001$) (table 4). Globally, 15 (24.2%) subjects had lymphatic and/or distant metastases, and only 3 cases of death related to CMs were found.

Diffuse folliculotropism (P value < .001), presence of atypical melanocytes into the isthmus (P value .003), and perifollicular involvement (P value < .001) correlated with CM recurrence. Other negative predictive factors included nodular subtype (P value .001), greater Breslow thickness (P value < .001), lymphovascular invasion (P value < .001), presence of mitoses (P value .001), and ulceration (P value

.017). Solar elastosis was observed in 88.7% of cases, underlining the importance of chronic UV damage in the HNR. Age at diagnosis, sex, primary anatomic site, and tumor-infiltrating lymphocytes were not significantly correlated with survival.

Table 1. Clinical and pathological features of 62 patients with primary head and neck melanoma correlated with the disease progression

Variables		Non Recurrence		Disease progression		P-value
		N	%	N	%	
Age-at diagnosis (years)	Median (range)	66.66 (25-91)		73.93 (56-88)		0.055
Sex	Females	21	87.5	3	12.5	0.088
	Males	26	68.4	12	31.6	
Primary tumor site	Scalp	5	55.6	4	44.4	0.308
	Neck	8	80.0	2	20.0	
	Face	34	79.1	9	20.9	
Tumor thickness (mm)	Median (range)	0.79 (0.2-5.5)		2.85 (0.9-8)		<0.001
Modified thickness (mm)	Median (range)	0.59 (0.2-3.0)		1.47 (0.9-2.6)		<0.001
	Nd	4		8		
Ulceration	Absent	43	81.1	10	18.9	0.017
	Present	4	44.4	5	55.6	
Mitotic rate	<1/mm2	35	89.7	4	10.3	0.001
	≥1/mm2	12	52.1	11	47.9	
Tumor type	LMM	17	77.3	5	22.7	0.001
	NM	5	38.5	8	61.5	
	SSM	25	92.6	2	7.4	
TILs	Absent/Nonbrisk	24	68.6	11	31.4	0.130
	Brisk	23	85.2	4	14.8	
Lymphovascular invasion	Absent	37	97.4	1	2.6	<0.001
	Present	5	33.3	10	66.7	
	Nd(not evaluable)	0	0	1	100	
Perifollicular	Absent	39	100	0	0	<0.001
	Present	8	34.8	15	65.2	
	Diffuse	15	53.6	13	46.4	0.001
Folliculotropism	Focal	26	96.3	1	3.7	
	Destroyed	2	100	0	0	
	Absent	2	100	0	0	
	Nd	2	75	1	33.3	
Folliculotropism depth	Isthmus	25	80.6	6	19.4	0.003
	Infundibulum	17	94.4	1	5.6	
	Buldge	1	50	1	50	
	Distruction	4	57.1	7	63.6	

Table 2. Numbers of cases of folliculotropism and melanoma subtype, location, and Breslow thickness.

	Diffuse folliculotropism	Focal folliculotropism	Not present or destroyed	Follicles present but not involved
Subtype				
SSM	10	15	2	0
LMM	8	12	0	2
NM	10	0	3	0
Location				
Face	17	22	3	1
Scalp	6	1	1	1
Neck	5	4	1	0
Breslow (mm)				
	0.2 to 8 (mean 1.93)	0.2 to 1.1 (mean 0.47)	0,2 to 5,5 (mean 2.29)	

Table 3. Numbers of cases of folliculotropism according to morphology and melanoma subtype, location, and Breslow thickness

	Isthmus	Infundibulum	Buldge	Distruction
Subtype				
SSM	15	12	0	0
LMM	14	6	2	0
NM	2	0	0	11
Location				
Face	21	12	2	8
Scalp	4	2	0	3
Neck	6	4	0	0
Breslow (mm)				
	0.2 to 3.0 (mean 0.83)	0.2 to 1.0 (mean 0.41)	0.6 to 0.9 (mean 0.75)	2.0 to 8.0 (mean 4.00)

Table 4. Table of discordant cases between traditional and follicular Breslow thickness.

Number of cases	Traditional Breslow	Folllicular Breslow
5	0.2	0.3
1	0.2	0.4
2	0.3	0.4
1	0.3	0.5
2	0.5	0.6
1	0.5	0.7
1	1.2	1.4
1	1.6	1.7
1	2.5	2.6

DERMOSCOPIC ANALYSIS AND CORRELATION WITH FOLLICULOTROPISM

Materials and methods

Cases of subjects with HNR LMs and LMMs diagnosed between January 2005 and December 2014 were examined (approved study protocol DERM-MTC 2017). Lesions with a preponderance of smaller cells at histology without solar elastosis or presence of single elastic fibers only, were diagnosed as a lentiginous pattern of SSM and were excluded, as well as mucosal and ocular CMs. Patients' data were collected, including sex, age at diagnosis, the anatomic site and CM characteristics. Anatomic areas of the excised CMs were classified as 1) scalp, 2) face (forehead, nose and cheeks) and 3) neck. LMs/LMMs of the ears and eyelids were excluded to the low density of HFs and those subjects treated with Mohs surgery, as horizontal slides did not provide sufficient information on HFs. Dermatoscopic images (x 20 and x 40 magnification) were analyzed and seven dermatoscopic parameters were evaluated, including (1) light/dark brown pseudonetwork, (2) dark/grey rhomboidal structures, (3) grey circles, (4) asymmetric pigmented follicular openings, (5) blue dots, (6) light brown structureless areas and (7) red areas (fig. 8 and 9). H&E slides of primary and recurrent LMs/LMMs were reviewed by three expert dermatopathologists (DM, CM, JLP), while prospective diagnoses were confirmed. Folliculotropism was evaluated in the selected specimens and the distribution of the melanocytes was classified as (1) absent – no involvement; (2) focal – involvement (< 3 HFs/sample); (3) diffuse – involvement (≥3 HFs/sample) (fig. 10 and 11). The level of involvement in the HF was categorized as extending into the (1) infundibulum; (2) isthmus; (3) bulb. The grade of solar elastosis was classified as (1) absent; (2) mild – increased elastic fibers in the upper dermis, with incremented width; (3) moderate-thickened elastic fibers with a disarranged orientation in the upper dermis; and (4) severe – serpiginous and thickened elastic fibers, constituting most of the upper dermis.

Fig. 8. Clinical (a, c) and dermatoscopic presentation (b, d) of a lentigo maligna melanoma showing atypical dermatoscopic features: asymmetric pigmented follicular openings (green arrow), grey circles (yellow arrow) and red areas (red arrow).

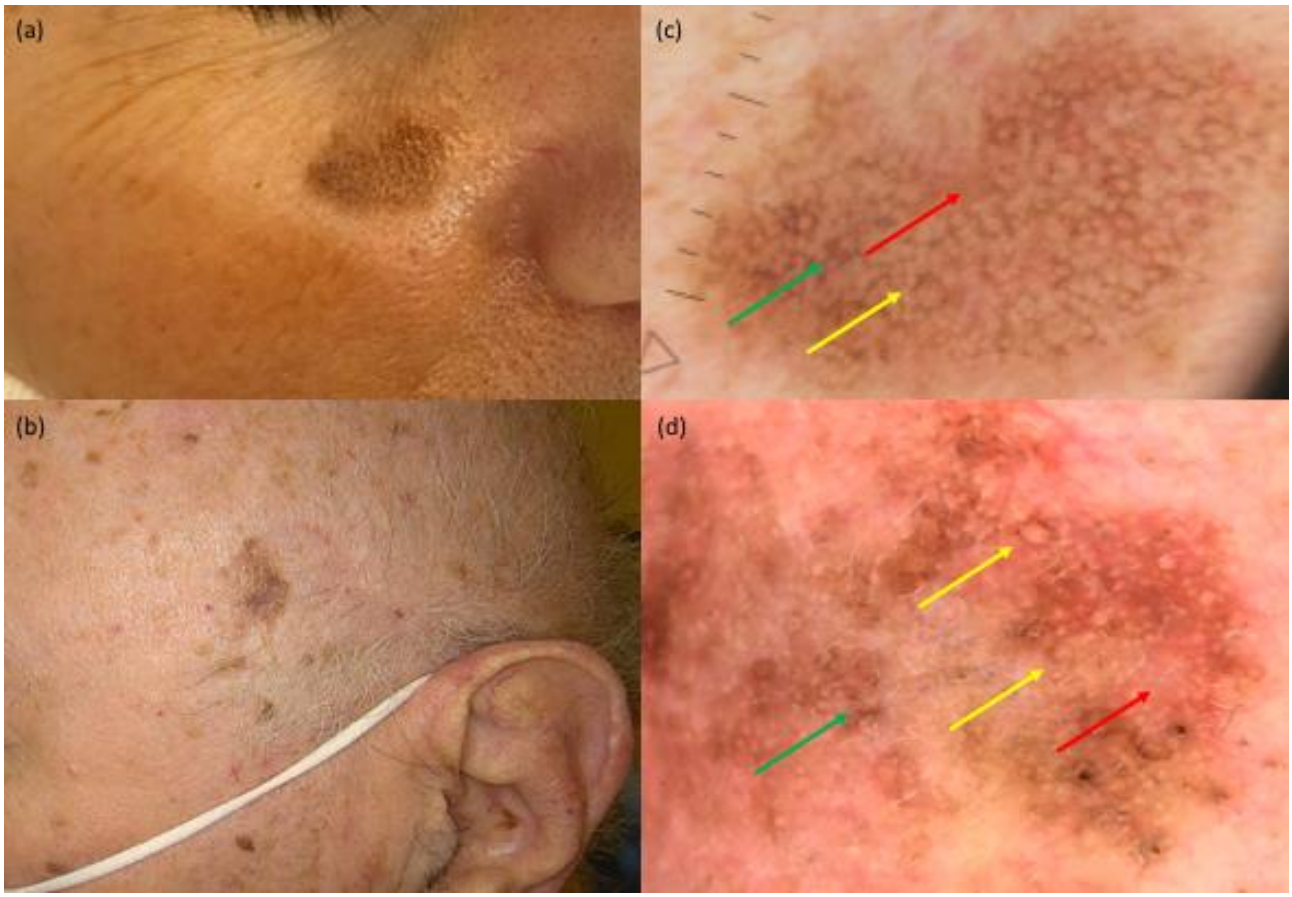

Fig. 9. Clinical (a, c) and dermatoscopic (b, d) presentations of a lentigo maligna melanoma showing light/dark brown pseudonetwork (dark blue arrow), structureless areas (yellow arrow), asymmetric pigmented follicular openings (light blue arrow), grey circles (red arrow) and dark rhomboidal structures (green arrow).

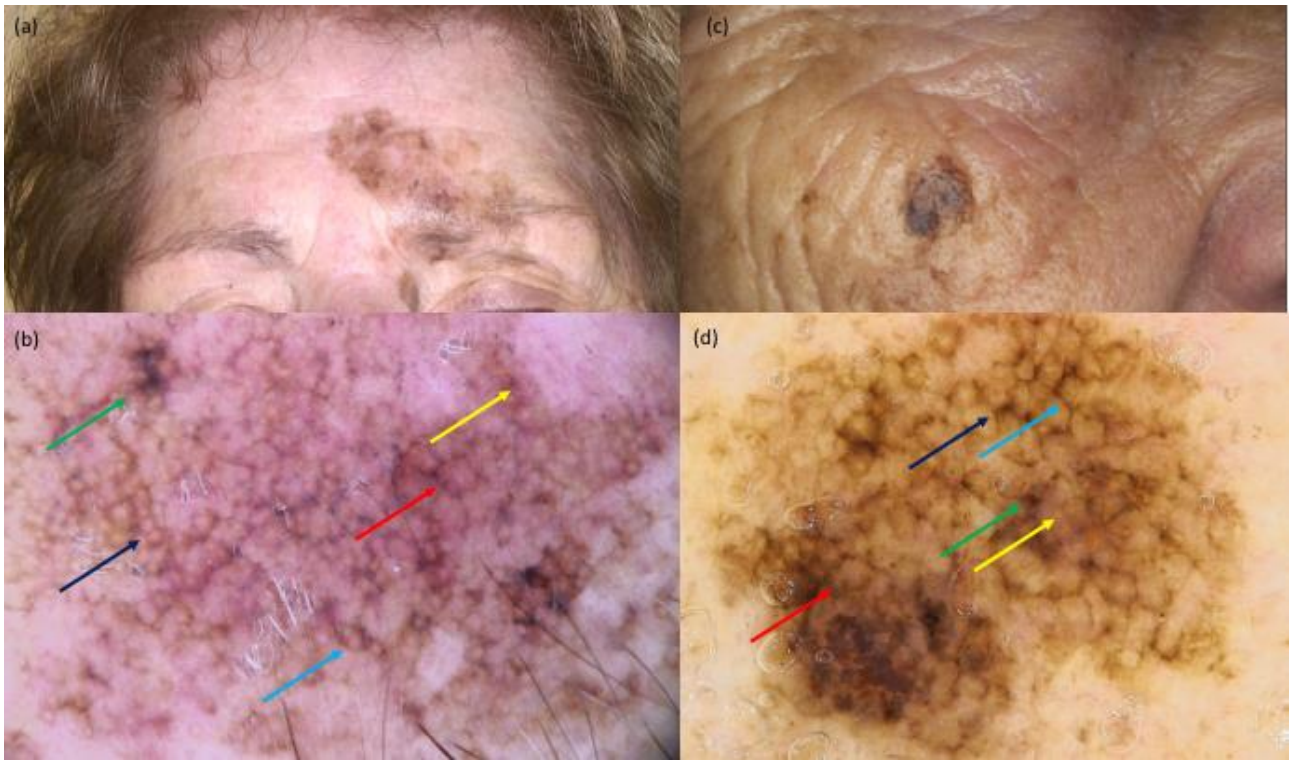

Fig. 10. Histopathological slide of a lentigo maligna (hematoxylin-eosin stain, original magnification x 10). It shows a proliferation of atypical melanocytes in the epithelium of the follicular unit.

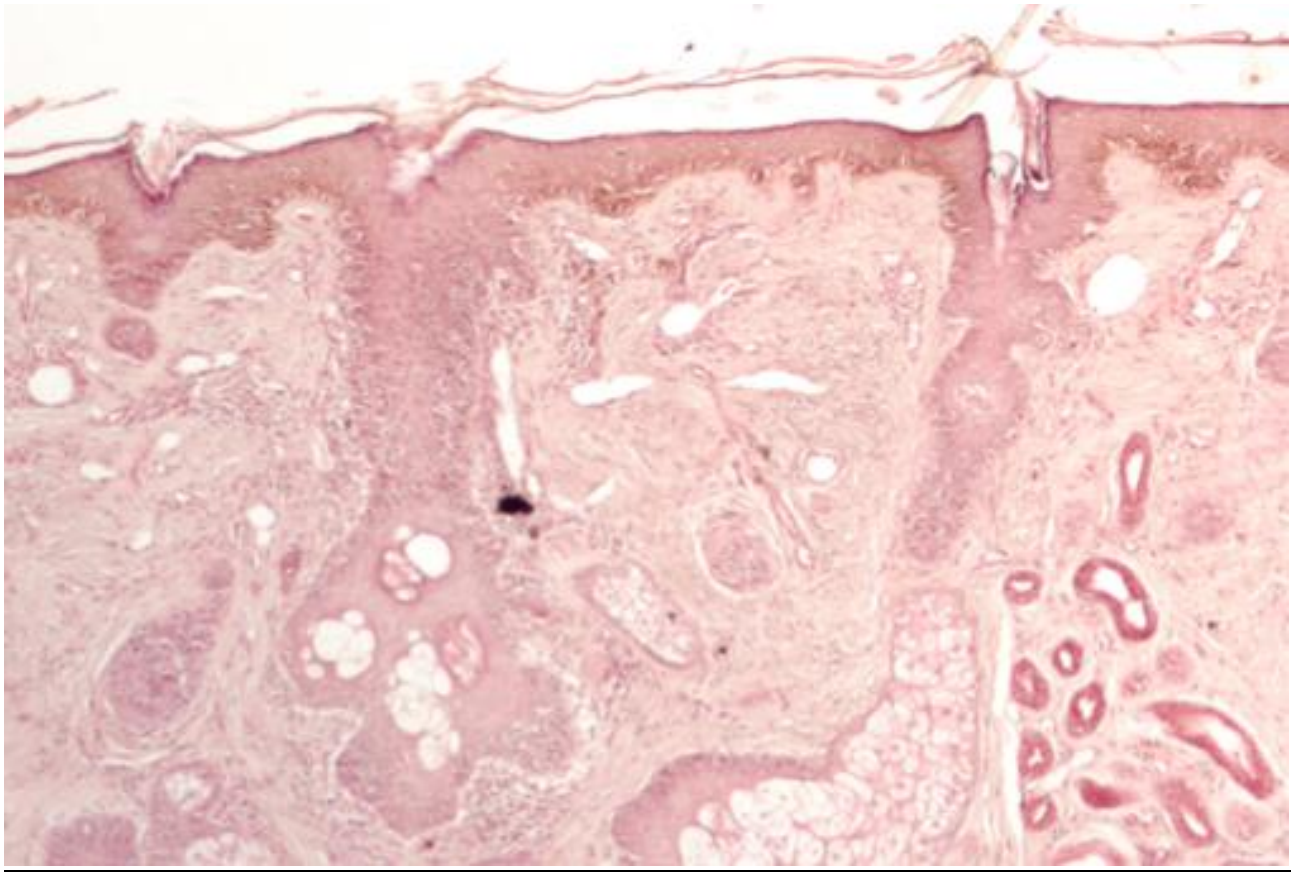

Fig. 11. Histopathological slides of a lentigo maligna melanoma (hematoxylin-eosin stain, original magnification x10 (a), x20 (b)). They show a proliferation of atypical melanocytes in the dermis and in the epithelium of the infundibulum and isthmus of the follicular unit.

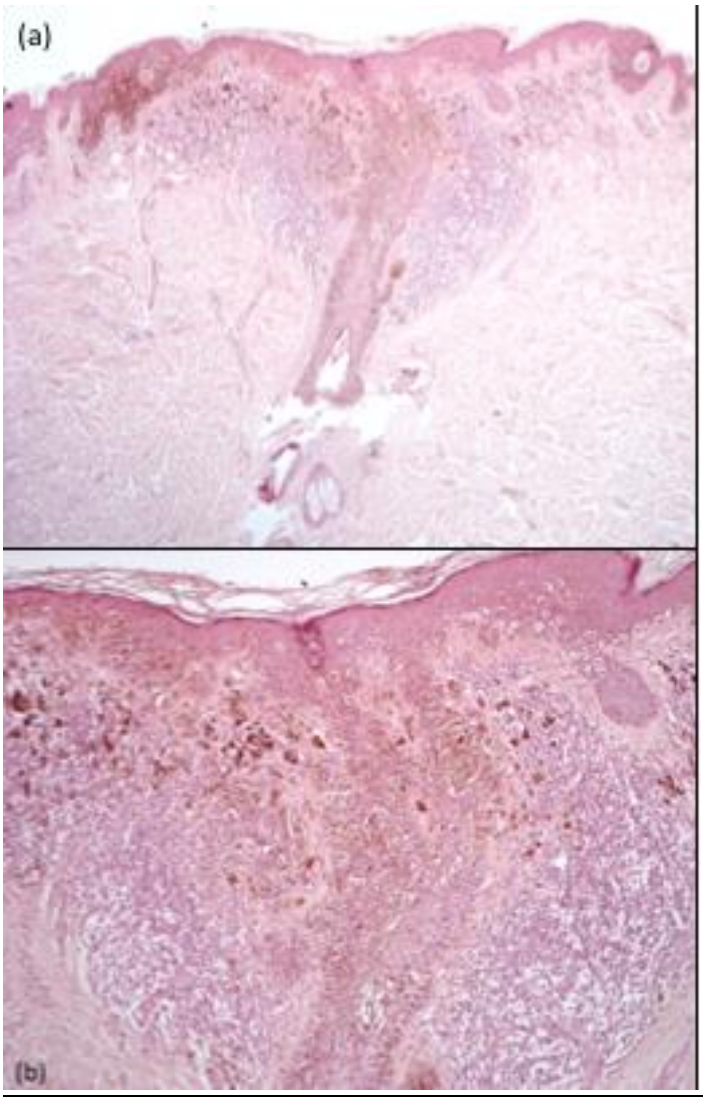

Statistical Analysis

Numerical data were expressed as mean and standard deviation or median and range, as appropriate. Qualitative data were shown as frequency and percentage. The chi-square test (Fisher's exact test) was used to examine the relation between qualitative variables, whilst statistical differences for continuous variables for the two groups were examined using the Student's t test. Multivariate

analysis was performed using logistic regression for the significant factors identified with univariate analysis; lesions were grouped according to infundibular, isthmic/bulge or bulb involvement. The results were shown as odds ratio (OR) with a 95% confidence interval (CI). A P value < 0.05 was considered significant.

Results

Globally, 25 LMs and 73 LMMs entered the study. In the majority of the cases, subjects were male (61%) and most lesions were located on the face (69%). Specific dermatoscopic features were statistically different between LM and LMM. Light/dark brown pseudonetwork and asymmetric pigmented follicular opening were associated with LM (92% and 92%, respectively), while they were detected in just around half of the LMM (p=0.004 and p<0.001, respectively). Almost all the blue dots registered were observed in LMM (20% vs 4% in LM, p=0.016). Severe solar elastosis was found in more than two-thirds of LMs. The mean Breslow thickness in the LMM group was 1.2 mm (±2.17; range 0.1–10). Tumor infiltrating lymphocytes were detected in 62% of the cases (n = 45), ulceration in 5 samples and regression in almost 1/3 of the specimens (n=22; 30%). Demographic characteristics, dermatoscopic and histopathological features are outlined according to histopathology diagnoses in tables 5 and 6. The correlation of dermatoscopic elements with LM follicular distribution and level of involvement showed that grey circles (44%) indicated an isthmic or bulb level of involvement, whilst being totally absent in the infundibular LM lesions (p=0.041) (fig. 8). A analogue trend, but not statistically significant, was seen with the grey rhomboidal structures; mainly absent in infundibular LMs, and more represented in the isthmic and bulb LMs (p=0.082). Blue dots were detected in 1 case of LM, which was one of the two LMs with bulb involvement (p=0.005) (table 7). None of the dermatoscopic parameters correlated with LM follicular distribution (table 8).

In the group of LMMs, the level of follicular involvement was not correlated with any of the dermatoscopic parameteres (table 7), but with the distribution of neoplastic cells in the HFs. Light/dark brown pseudonetwork and light brown structureless areas were associated to a diffuse

distribution (P < 0.001 and P = 0.001, respectively), grey circles indicated either focal or diffuse distribution (P < 0.001) (fig. 9) (table 8).

Table 5. Clinical, dermoscopic and histopathological evaluations of lentigo maligna included in the study.

LM (n = 25)		
Age, *median ±SD (range)*	72 ±14.5 (32 – 88)	
Localization of LM, *n (%)*	*Face*	22 (88)
	Neck	2 (8)
	Scalp	1 (4)
Dermoscopic features, *n (%)*:		
Light/dark brown pseudonetwork	*Present*	23 (92)
	Missing	2 (8)
Dark rhomboidal structures	*Present*	12 (48)
	Absent	10 (40)
	Missing	3 (12)
Grey circles	*Present*	11 (44)
	Absent	12 (48)
	Missing	2 (8)
Asymmetric pigmented follicular openings	*Present*	23 (92)
	Missing	2 (8)
Blue dots	*Present*	12 (48)
	Absent	11 (44)
	Missing	2 (8)
Light brown structureless areas	*Present*	16 (64)
	Absent	7 (28)
	Missing	2 (8)
Red areas	*Present*	12 (48)
	Absent	11 (44)
	Missing	2 (8)
Histopathological features, *n (%)*:		
Solar elastosis	*Mild*	4 (16)
	Moderate	4 (16)
	Severe	17 (68)
Folliculotropism - distribution	*Absent*	1 (4)
	Focal	11 (44)
	Diffuse	12 (48)
	Not assessable	1 (4)
Folliculotropism - level of involvement	*Infundibular*	7 (28)
	Isthmic	14 (56)
	Bulb	2 (8)
	Not assessable	2 (8)

Table 6. Clinical, dermoscopic and histopathological evaluations of lentigo maligna melanoma included in the study.

LMM (n = 73)		
Age, *median ±SD (range)*	69 ±13.7 (24 – 91)	
Localization of LMM, *n (%)*	*Face*	46 (63)
	Neck	14 (19)
	Scalp	13 (18)
Dermoscopic features**, *n (%)*:		
Light/dark brown pseudonetwork	*Present* *Absent*	38 (72) 15 (28)
Dark rhomboidal structures	*Present*	24 (45)
	Absent	29 (55)
Grey circles	*Present*	33 (62)
	Absent	20 (38)
Asymmetric pigmented follicular openings	*Present*	31 (58)
	Absent	22 (42)
Blue dots	*Present*	15 (28)
	Absent	38 (72)
Light brown structureless areas	*Present*	35 (66)
	Absent	18 (34)
Red areas	*Present*	25 (47)
	Absent	28 (53)
Histopathological features, *n (%)*:		
Breslow thickness, *median ±SD (range)*	1.3 ± 2.2 (0.1 – 10)	
Folliculotropism - distribution	*Absent*	2 (3)
	Focal	30 (40)
	Diffuse *Destroyed*	27 (37) 7 (10)
	Not assessable	7 (10)
Folliculotropism - level of involvement	*Infundibular*	7 (28)
	Isthmic	14 (56)
	Bulb	2 (8)
	Not assessable	2 (8)

Table 7. Correlation between dermoscopic features and level of involvement of malignant melanocytes in the follicular units.

		Level of involvement LMM								**Level of involvement LM**							
		Infundibular n=15		*Isthmic n=20*		Bulb n=3		Missing n=35	p-value	Unable to be evaluated n=2		*Infundibular n=7*		*Isthmic n=14*		Bulb n=2		p-value
Dermoscopic features:		n	%	n	%	n	%	n		n	%	n	%	n	%	n	%	
Light/dark brown pseudonetwork	*Absent*	0	*0*	3	*15*	0	*0*	12	0.284	0	*0*	0	*0*	0	*0*	0	*0*	-
	Present	10	*67*	13	*65*	2	*67*	13		2	*100*	6	*86*	13	*93*	2	*100*	
	Missing	5	*33*	4	*20*	1	*33*	10		0	*0*	1	*14*	1	*7*	0	*0*	
Dark rhomboidal structures	*Absent*	3	*20*	9	*45*	0	*0*	17	0.188	0	*0*	5	*71*	5	*36*	0	*0*	0.082
	Present	7	*47*	7	*35*	2	*67*	8		2	*100*	1	*14*	7	*50*	2	*100*	
	Missing	5	*33*	4	*20*	1	*33*	10		0	*0*	1	*14*	2	*14*	0	*0*	
Grey circles	*Absent*	3	*20*	3	*15*	0	*0*	14	0.592	0	*0*	6	*86*	5	*36*	1	*50*	0.041
	Present	7	*47*	13	*65*	2	*67*	11		2	*100*	0	*0*	8	*57*	1	*50*	
	Missing	5	*33*	4	*20*	1	*33*	10		0	*0*	1	*14*	1	*7*	0	*0*	
Asymmetric pigmented follicular openings	*Absent*	4	*27*	7	*35*	0	*0*	11	0.489	0	*0*	0	*0*	0	*0*	0	*0*	-
	Present	6	*40*	9	*45*	2	*67*	14		2	*100*	6	*86*	13	*93*	2	*100*	
	Missing	5	*33*	4	*20*	1	*33*	10		0	*0*	1	*14*	1	*7*	0	*0*	
Blue dots	*Absent*	7	*47*	12	*60*	0	*0*	19	0.99	2	*100*	6	*86*	14	*100*	1	*50*	0.005
	Present	3	*20*	4	*20*	2	*67*	6		0	*0*	0	*0*	0	*0*	1	*50*	
	Missing	5	*33*	4	*20*	1	*33*	10		0	*0*	1	*14*	0	*0*	0	*0*	
Light brown structureless areas	*Absent*	2	*13*	2	*10*	0	*0*	14	0.726	2	*100*	2	*29*	3	*21*	0	*0*	0.628
	Present	8	*53*	14	*70*	2	*67*	11		0	*0*	4	*57*	10	*71*	2	*100*	
	Missing	5	*33*	4	*20*	1	*33*	10		0	*0*	1	*14*	1	*7*	0	*0*	
Red areas	*Absent*	5	*33*	9	*45*	0	*0*	14	0.325	2	*100*	4	*57*	4	*29*	1	*50*	0.332
	Present	5	*33*	7	*35*	2	*67*	11		0	*0*	2	*29*	9	*64*	1	*50*	
	Missing	5	*33*	4	*20*	1	*33*	10		0	*0*	1	*14*	1	*7*	0	*0*	

Table 8. Correlation between dermoscopic features and distribution of malignant melanocytes in the follicular units

		Distribution LMM											**Distribution LM**								
		Absent n=2		Focal n=30		Diffuse n=27		Unable to be evaluated n=7		Missing n=7		p-value	*Absent n=1*		Focal, n=11		Diffuse, n=12		Unable to be evaluated n=1		p-value
Dermoscopic features:		n	*%*	n	*%*	n	*%*	n	*%*	n	*%*		n	*%*	n	*%*	n	*%*	n	*%*	
Light/dark brown pseudonetwork	*Absent*	*0*	*0*	1	*3*	6	*22*	6	*86*	2	*29*	<0.001	*0*	*0*	0	*0*	0	*0*	0	*0*	-
	Present	*2*	*100*	16	*53*	18	*67*	0	*0*	2	*29*		*1*	*100*	11	*100*	10	*83*	1	*100*	
	Missing	*0*	*0*	13	*43*	3	*11*	1	*14*	3	*43*		*0*	*0*	0	*0*	2	*17*	0	*0*	
Dark rhomboidal structures	*Absent*	*1*	*50*	6	*20*	14	*52*	6	*86*	2	*29*	0.052	*0*	*0*	7	*64*	3	*25*	0	*0*	0.167
	Present	*1*	*50*	11	*37*	10	*37*	0	*0*	2	*29*		*1*	*100*	3	*27*	7	*58*	1	*100*	
	Missing	*0*	*0*	13	*43*	3	*11*	1	*14*	3	*43*		*0*	*0*	1	*9*	2	*17*	0	*0*	
Grey circles	*Absent*	*2*	*100*	2	*7*	9	*33*	6	*86*	1	*14*	<0.001	*0*	*0*	8	*73*	4	*33*	0	*0*	0.200
	Present	*0*	*0*	15	*50*	15	*56*	0	*0*	3	*43*		*1*	*100*	3	*27*	6	*50*	1	*100*	
	Missing	*0*	*0*	13	*43*	3	*11*	1	*14*	3	*43*		*0*	*0*	0	*0*	2	*17*	0	*0*	
Asymmetric pigmented follicular openings	*Absent*	*1*	*50*	4	*13*	9	*33*	6	*86*	2	*29*	0.012	*0*	*0*	0	*0*	0	*0*	0	*0*	-
	Present	*1*	*50*	13	*43*	15	*56*	0	*0*	2	*29*		*1*	*100*	11	*100*	10	*83*	1	*100*	
	Missing	*0*	*0*	13	*43*	3	*11*	1	*14*	3	*43*		*0*	*0*	0	*0*	2	*17*	0	*0*	
Blue dots	*Absent*	*2*	*100*	13	*43*	14	*52*	6	*86*	3	*43*	0.143	*1*	*100*	11	*100*	10	*83*	1	*100*	0.745
	Present	*0*	*0*	4	*13*	10	*37*	0	*0*	1	*14*		*0*	*0*	0	*0*	1	*8*	0	*0*	
	Missing	*0*	*0*	13	*43*	3	*11*	1	*14*	3	*43*		*0*	*0*	0	*0*	1	*8*	0	*0*	
Light brown structureless areas	*Absent*	*0*	*0*	2	*7*	8	*30*	6	*86*	2	*29*	0.001	*1*	*100*	4	*36*	1	*8*	1	*100*	0.081
	Present	*2*	*100*	15	*50*	16	*59*	0	*0*	2	*29*		*0*	*0*	7	*64*	9	*75*	0	*0*	
	Missing	*0*	*0*	13	*43*	3	*11*	1	*14*	3	*43*		*0*	*0*	0	*0*	2	*17*	0	*0*	
Red areas	*Absent*	*1*	*50*	8	*27*	12	*44*	5	*71*	2	*29*	0.466	*1*	*100*	5	*45*	4	*33*	1	*100*	0.484
	Present	*1*	*50*	9	*30*	12	*44*	1	*14*	2	*29*		*0*	*0*	6	*55*	6	*50*	0	*0*	
	Missing	*0*	*0*	13	*43*	3	*11*	1	*14*	3	*43*		*0*	*0*	0	*0*	2	*17*	0	*0*	

FREQUENCY OF SOMATIC MUTATIONS IN HEAD AND NECK MELANOMA

Materials and methods

A total of 76 cases of primary HNR CMs diagnosed from January 2005 to June 2017 were evaluated and 19 cases with the molecular assays and a 5-year follow-up were included to correlate the mutational status with the clinicopathological features and the disease progression (table 9). The study

was approved by the Ethical Committee of Saint Orsola-Malpighi Hospital, Bologna University (CE study MTC/2017/U/Tess). Blocks of formalin-fixed, paraffin-embedded CM tissue were obtained and reviewed from the Laboratory of Dermatopathology, University of Bologna. Molecular assays were performed at the Laboratory of Oncologic and Transplantation Molecular Pathology of Bologna University. DNA extraction was performed from 10-μm sections of paraffin-embedded tissue to obtain a higher percentage of enrichment in CM cells. The extraction was performed using the QIAampDNA FFPE Tissue kit. Concentration of extracted DNA was assessed by real-time PCR using the Quantifiler kit. Mutation analyses in oncogenes *BRAF* (exon 15), *c-Kit* (exons 9, 11, 13, and 17), and *NRAS* (exons 2, 3) were performed using the direct sequencing method. After PCR reaction, amplified DNA was purified using MinElute PCR purification kit. Sequencing was performed using the Big Dye Terminator sequencing kit version 3.0 by applying in two separate reactions forward and reverse primers. Sequencing analysis was performed using the automated sequencer, and sequencing results were interpreted with chromas software version 1.45.

Table 9. Demographic and clinicopathological data of patients with head and neck melanomas.

Age at diagnosis	(n = 19)
≤60	6 (31.6%)
61–80	11 (57.9%)
>80	2 (10.5%)
Patient's sex	
Male	13 (68.4%)
Female	6 (31.6%)
Histological type	
SSM	4 (21.1%)
NM	8 (42.1%)
LMM	7 (36.8%)
Breslow tumor thickness	
T1: ≤0.8 mm	11 (57.9%)
T2: 0.9–2 mm	5 (26.3%)
T3: 2.01–4 mm	3 (15.8%)
T4: ≥4 mm	0
Metastases no. (%)	
Absent	14 (73.7%)
Lymph nodes	4 (21%)
Visceral	1 (5.3%)
Unknown	0

Results

Nodular CM was the most frequent histopathologic subtype (42.1%): four cases were located in the neck, three in the scalp, and one on the face (table 9). All the analyzed nodular lesions revealed the absence or a less-pronounced intraepidermal component extending laterally to a maximum of three epidermal rete ridges relative to the invasive component. LMM represented 36.8% of cases: two cases were located in the scalp, three on the face, and two cases on the nose. LMM did not show an evident pagetoid spread and consisted of a contiguous proliferation of atypical neoplastic cells at the lower levels of the epidermis. Folliculotropism was typically seen. SSM represented 21.1% of cases, all detected on the face. Atypical melanocytes were observed at all levels of the epidermis, with single or small aggregates present in the stratum corneum or granulosum (“pagetoid growth”). Neoplastic

cells both of the in situ and the invasive component were epithelioid with large amounts of cytoplasm with wide atypical vesicular nuclei with prominent nucleoli, and often containing melanin pigment. No desmoplastic CMs were registered. Solar elastosis was observed in 90% of cases revealing a chronic sun exposure. *BRAF* mutations were observed in five cases (26.3%): two SSM, associated with vertical growth, displayed a *V600E* mutation (table 10,11). The *V600K* mutation was noticed in a NM and in a LMM, while *K601E* mutation in one LMM. *NRAS p.Q61L* mutation was observed in a NM of the scalp, when the other cases were wild type for the investigated gene mutations.

Table 10. Results of *BRAF*, *NRAS*, and *c-Kit* molecular analyses among patients affected by head and neck melanoma.

Case number	BRAF status	NRAS status	c-Kit status
1	WT	WT	WT
2	WT	**p.Q61L**	Not amplified
3	WT	WT	WT
4	**p.K601E**	WT	WT
5	**p. V600E**	WT	WT
6	**p. V600K**	WT	WT
7	**p. V600K**	WT	Not amplified
8	**p. V600E**	WT	WT
9	WT	WT	WT
10	WT	WT	WT
11	WT	WT	WT
12	WT	WT	WT
13	WT	WT	WT
14	WT	WT	Not amplified
15	WT	WT	WT
16	WT	WT	WT
17	WT	WT	WT
18	WT	WT	WT
19	WT	WT	WT

Table 11. Results *of BRAF, NRAS* and *Kit* molecular analyses of patients affected by head and neck melanoma in COSMIC database.

	BRAF status	*NRAS* status	*Kit* status
LMM	3/31 p.V600K p.L587 p.E586K	4/22 p.Q61K p.Q61L p.Q61R (x2)	0/0
NM	5/18 p.V600E (x5)	2/18 p.Q61R p:Q61E62delins HK	1/1 p.P524L
SSM	4/4 p. V600E (x2) p-V600X p.L597R, p.G593S (same sample)	0/0 WT WT	0/0 WT WT

ASSOCIATION OF MIR-146A-5P WITH CUTANEOUS MELANOMA PROGNOSTIC FEATURES

Materials and Methods

Formalin fixed-paraffin embedded specimens from 129 subjects with CMs were evaluated. Acral lentiginous CMs, CMs in situ, CMs on nevus were excluded. The study protocol was approved by the Ethics Committee CE-AVEC (417/2018/Sper/AOUBo). Expert dermatopathologists defined only the area with morphological defined neoplastic cells from a 3 µm stained H&E slides and RNA was isolated from neoplastic cells with miRNeasy FFPE kit (Qiagen, Hilden, Germany). Deparaffinization was done with xylene followed by an ethanol wash. RNA quality check was

assessed by NanoGenius Spectrophotometer, (ONDA Spectrophotometer). Contamination of protein (260\280 ratio) was also checked. RNA was stored at -80°C.

RNA samples were converted to cDNA using miRCURY LNA RT kit (Qiagen, catalog number 339340). Reverse-transcription (RT) was performed in a 10 μL reaction starting from 10 ng of each total RNA samples. cDNA samples were stored at −20 °C. RT-quantitative PCR (qPCR) was performed using 4 μL of diluted cDNA for each sample, 5 μL of miRCURY LNA SYBER Green PCR mix (Qiagen, catalog number 339346) and 1 μL of primer hsa-miR-146a-5p (Qiagen, catalog number YP00204688) from miRCURY LNA miRNA PCR Assays (Qiagen, catalog number 339306). SNORD44 (Qiagen, catalog number YP00203902) expression was also tested. Normalized miR-146a-5p expression was calculated using SNORD44, a small nucleolar RNA, as reference gene. Each assay was tested in triplicate under the following thermal cycling conditions: 95°C for 10 minutes, 39 cycles of 95°C for 10 seconds, 60°C for 1 minute. RT-qPCR data were analyzed with Bio-Rad CFX Manager software.

Statistical analysis

Starting from data obtained by CFX Manager software, the levels of miR-146a-5p were calculated. MiRNA level was described as a value called Cycle threshold (Ct) which is defined as the amount of cycles needed for the fluorescent signal to cross the threshold line. Threshold line was established to eliminate background noise. Ct levels are inversely proportional to the amount of target nucleic acid in the initial template. RT-qPCR data were reported as relative expression quantification; hence Ct of the target miRNA was compared with the reference gene, using the $2^{-(\Delta Ct)}$ method.[100]

For all categorical variables, differences across the groups were analyzed using Mann-Whitney or unpaired t-test according to D'Agostino-Pearson Test for normality. The correlation of miRNA profile with specific histo-pathological elements was defined as significant for values of two-sided $P \leq 0.05$. Statistical analysis was performed using Graphpad Prism 8 (Graphpad Prism Software).

Results

Globally, 143 FFPE CMs specimens were evaluated: 90 SSMs, 28 LMMs and 25 NMs. Patients' characteristics are reported in table 12. cDNA was extracted for all specimens and performed RT-qPCR to assess the miRNA expression in all CMs. The correlation between miR-146a-5p expression and CM histopathological parameters that are important in CM prognosis (mitotic rate, ulceration and regression) was assessed. A significantly greater miRNA expression was detected in CMs with a greater mitotic rate ($\geq 1/mm^2$) (fig. 12a) as well as in ulcerated CMs with respect to those without ulceration (fig. 12b). No difference in miR-146a-5p expression was observed when we evaluated regression in all CMs subtypes (fig. 13a), whilst a higher expression was observed in the LMM subtype presenting regression (fig. 13b). The correlation between miR-146a-5p expression and CM body area was analyzed (fig. 14). Considering the recognized association of miR-146a-5p with Breslow thickness, the selected cases were stratified on the basis of BT ($\geq <$ 0.8 mm) and CM area, specifically the HNR vs the other sites together (OBL).[59] MiR-146a-5p expression resulted lower in HNR CMs with BT $\geq$0.8 mm (fig. 14).

Table 12. Demographic, histological and clinical characteristics of the reported cases.

	SSM	LMM	NM
Total (n°)	90	28	25
Gender (n°)			
Male	60	13	20
Female	30	15	5
Age			
< 50 years	32	2	8
≥ 50 years	58	26	17
Breslow Thickness (n°)			
< 0.8 mm	54	23	1
≥ 0.8 mm	36	5	24
Tumor location (n°)			
Head and neck	5	22	1
Other body areas	85	6	24
Ulceration (n°)			
Present	10	0	9
Absent	80	26	14
Not available		2	2
Mitosis (n°)			
< 1/mm^2	63	20	6
≥ 1/mm^2	26	5	17
Not available	1	3	2
Regression (n°)			
Present	44	8	4
Absent	46	17	20
Not available		3	1

Fig. 12. (a) Scatter plot showing a significant difference (p=0.015) in miR-146a-5p expression in samples with mitotic rate ≥ 1/mm2 and < 1/mm2. (b) The plot shows a higher significant miR-146a-5p expression in ulcerated samples compared to samples without presence of ulceration (p=0.004).

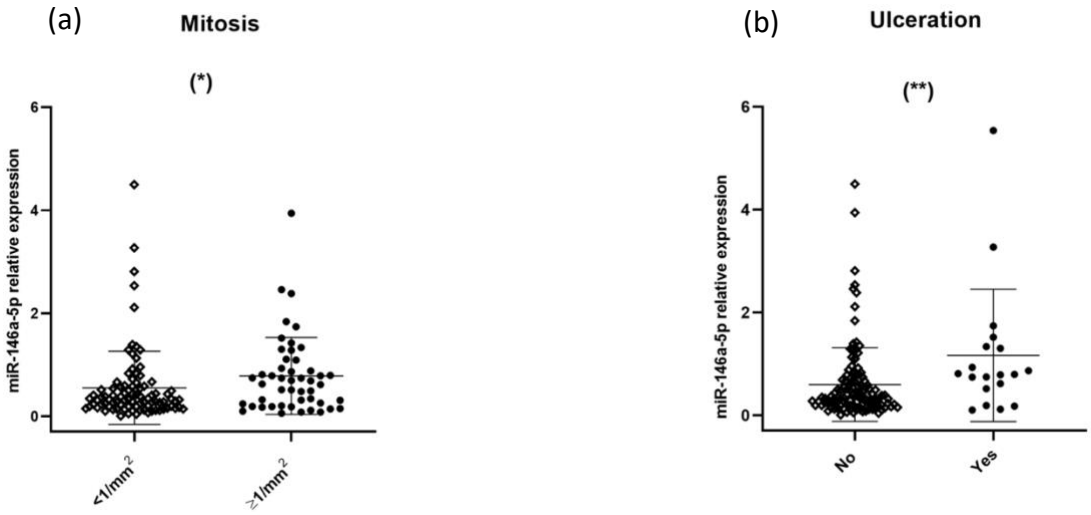

Fig. 13. Scatter plot: (a) miR-146a-5p did not shown different expression between samples with presence and absence of regression when considering all subtypes, but only in lentigo maligna melanoma subtype (b).

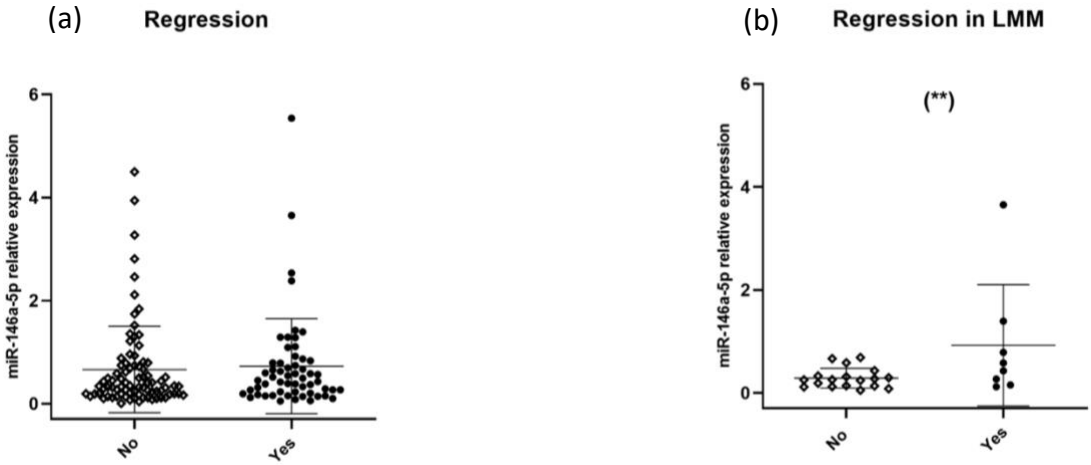

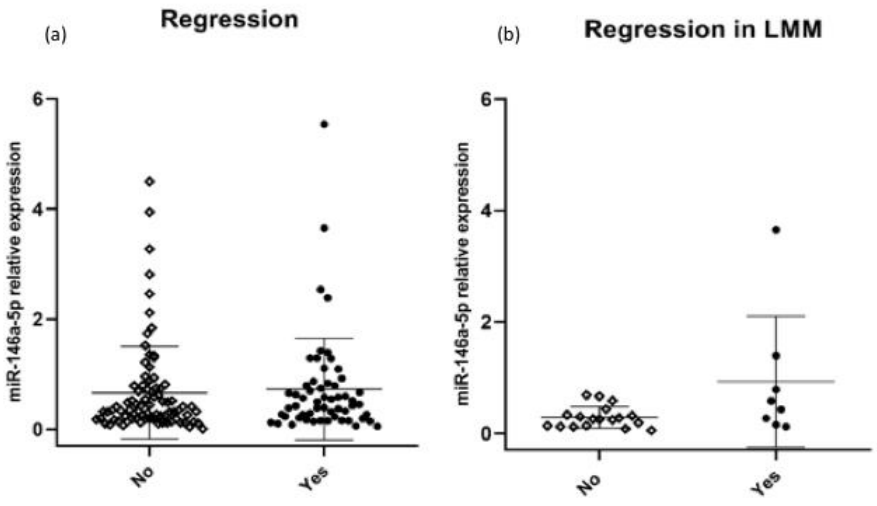
(a)
Regression
miR-146a-5p relative expression
6
4
2
0
No
Yes
(b)
Regression in LMM
miR-146a-5p relative expression
6
4
2
0
No
Yes

Fig. 14. Scatter plot graph representation of miR-146a-5p relative expression in cutaneous melanomas with head and neck localization and Breslow thickness ≥ or < 0.8 mm (HNL ≥ 0.8 mm, HNL < 0.8 mm) or with other body localization and Breslow thickness ≥ or < 0.8 mm (OBL ≥ 0.8 mm, OBL < 0.8 mm). The miR-146a-5p expression is significantly lower (p=0.0153) in melanoma with head and neck localization and Breslow thickness ≥ 0.8 mm compared to melanomas in other body sites with thickness ≥ 0.8 mm. Each miRNA was tested in triplicate by quantitative RT-PCR. Relative miRNA expression was normalized on SNORD44.

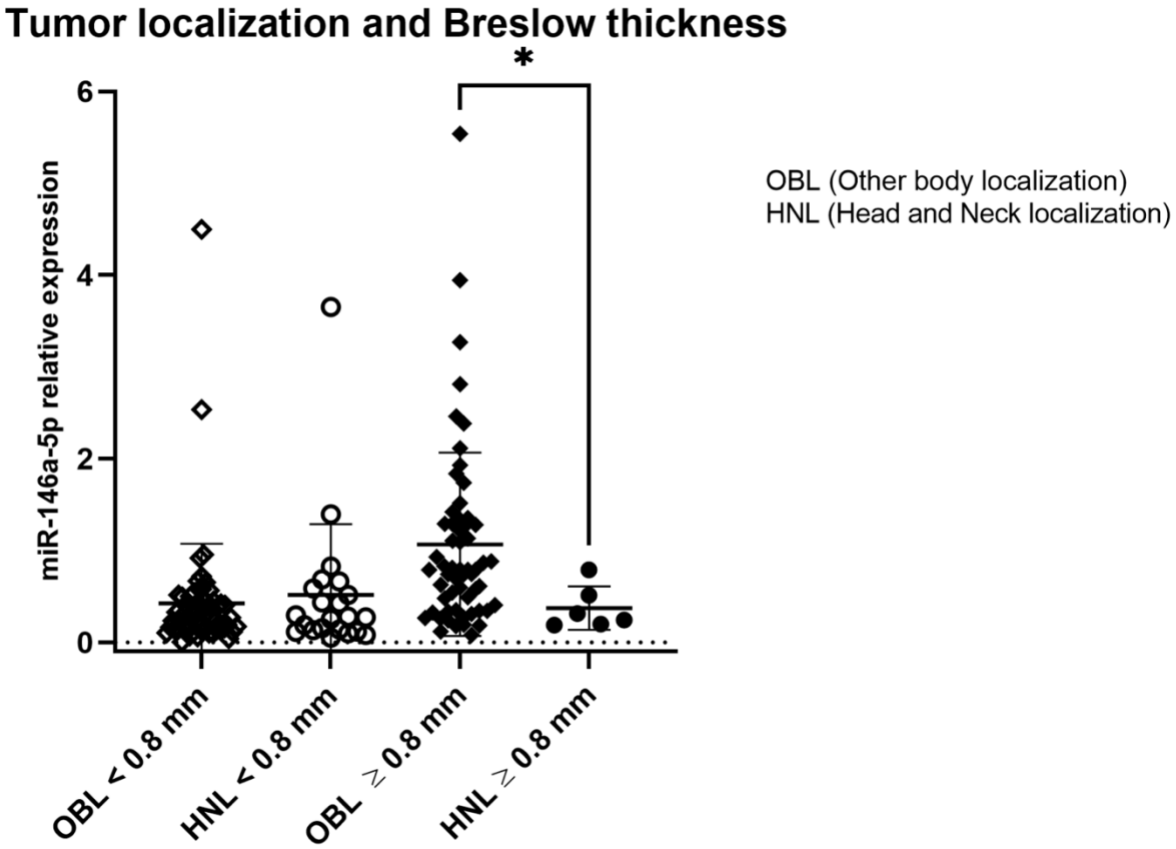

DISCUSSION

In the project both the distribution and the level of neoplastic HF involvement in HNR CMs has been analyzed: the folliculotropism was more frequent in the face compared to the neck and the scalp region. These findings are in line with the high HF density in this area. An original finding is the statistically significant correlation of the diffuse subtype, perifollicular involvement, and localization of neoplastic cells to the isthmus with the nodal and visceral metastases. These data could not be further correlated with prognosis because of the low number of CM-related deaths (n=3), and patients under immunologic or target therapies. The isthmus was the most frequent region of HF involvement, followed by the infundibulum. In only two cases of LMMs with a Breslow thickness of 0.2 and 0.4 mm we detected neoplastic cells at the outer root sheet at the bulb level. A previous report showed an infrequent occurrence of CM cells under the bulge into the bulb region, postulating a specific mechanism controlling the keratinocyte-melanocyte interaction at this level, according to the "bulge barrier theory".[48] It is noteworthy to point out that the follicular Breslow depth measurement[54] rather than the traditional Breslow thickness did not significantly modified our findings.

In the clinical practice dermoscopy is the most frequently applied diagnostic technology for the diagnosis and clinical management of pigmented lesions, but the correlation of dermatoscopic parameters and folliculotropism was not previously assessed.[101–111] Dermatoscopic features related to LM are not specific. *Grey circles* and *grey rhomboids* have been described as the most sensitive elements for the identification of LM, but they can be even observed in a number of other benign and neoplastic non-melanocytic lesions.[101,112] The presence of *grey circles* has been considered a differential feature for the diagnosis of LM from pigmented actinic keratosis, likely being the strongest indication of LM diagnosis.[101,113] In the present project, *grey circles* have been detected in almost half of LMs and have been statistically correlated with a deeper (isthmus and bulb) level of HF involvement; while in LMMs, they were associated with focal or diffuse folliculotropism. The findings are in line with the hypothesis that *grey circles* in LM probably arises from stem cells of the

HF bulge in the nearby isthmic region.[109,114] Solar elastosis, a histologic sign of actinic damage[115], was found in all LMs and graded as severe in 68% of the cases: this occurrence corroborates the pathogenetic role of UV radiations in LM and LMM and contributes to the understanding that CM has a stronger propensity for subclinical extension.

The majority of the HNR CMs evaluated in this project were BRAF and NRAS wild type. We compared our data with those published in COSMIC database.[116] In this database, we chose HNR CMs including all subtypes (desmoplastic, in situ, LM, nodular, not specified, SSM) and mutations of the assessed genes. BRAF mutations were registered in 35.8% (44/123), NRAS in 9% (7/78), and KIT in 9.2% (6/65) of cases. Evaluating our same histology (LMM, NM, and SSM), *BRAF* mutation was registered in 22.6% (12/53), *NRAS* in 15% (6/40), and *KIT* mutation was recorded only in one case of nodular CM; apparently, it was not assessed in other cases of LMM, NM, and SSM. *V600E BRAF* mutations were detected in 13.2% HNR CMs (5 NM and 2 SSM), and *non-V600E BRAF* mutations in 9.4% (table 11). In this projects, the results regarding *BRAF* mutations were substantially the same of COSMIC database; NRAS was lower, likely due to the difference in the UV exposure or in hair coverage.

In the last years the altered expression of miRNAs has been largely investigated in CM. In 2020, our group described that miR-21-5p and miR-146a-5p expression significantly correlated with Breslow thickness in SSMs, representing an objective molecular assay to corroborate standard Breslow thickness assessment.[59] MiR-146a-5p plays oncogenic role in CM and likely targeting *NUMB* gene, a repressor of NOTCH signaling, involved in melanocyte neoplastic degeneration.[117] Moreover, miR-146a-5p enhances cell migration and invasion by directly targeting *SMAD4*.[59] MiR-146a-5p has been shown to be one of the most over-expressed miRNAs in CM specimens compared to healthy skin.[118] MiR-146a-5p regulates *MAPK* signaling pathway that is involved in melanomagenesis and it was shown to be differentially regulated in metastatic versus primary CM.[118] However, miR-146a-5p is not fully univocal as its expression declines in circulating CM cells, inhibiting neoplastic spreading, downregulating *integrin alpha-V* precursor (*ITGAV*) and *Rho-associated protein kinase 1*

(*ROCK1*)[119,120]. Thus, MiR-146a-5p expression results modulated across the transition from in-situ to CM progression.[119]

Considering the above-mentioned background, we chose to determine the expression of miR-146a-5p in specific subtypes of CM, correlating it with specific CM features influencing the prognosis, including the HNR as well as regression, mitotic index and ulceration.

LMM is known to be the most represented histopathologic subtype of CM in the HNR, followed by SSM and NM.[15] This body area is usually exposed to a high cumulative UV exposure with subsequent solar elastosis and inflammation connected to DNA damage and reactive oxygen species (ROS) production.[15,59,121] ROS-induced inflammasomes control caspase-1-dependant production of pro-inflammatory interleukin (IL)1β and IL18 cytokines.[121] Furthermore, chronic inflammation due to actinic damage can induce an immune evasion process [122]. The literature reports that a wide subset of miRNAs, including miR-146a-5p, are significantly under-expressed after UV exposure, inducing an rise of immune evasive molecules such as PD-1, chemokines CCL2 and CCL8, and T cell co-stimulator ligand (ICOSLG also known B7H2).[123] MiR-146a-5p is implicated in inflammatory processes and plays a role as modulator of immune function, being involved in innate immunity.[124,125] Prior studies showed that a greater expression of miR-146 is associated to the negative regulation of the TLR/IL-1 receptor induced inflammatory response.[126] MiR-146a seems to provide a negative feedback of inflammation, inducing a down-regulation of *IRAK1* and *tumor necrosis factor receptor–associated factor 6* (*TRAF6*).[125]

Ulceration is defined as the full thickness lack of an undamaged epidermis above any part of the CM together with a host reaction. Ulceration has been assessed as an adverse prognostic parameter and it has been categorized as a T criterion staging system of the *American Joint Committee on Cancer* (AJCC) VIII edition.[127] Mitotic rate was a former T parameter in the AJCC VII edition but it was not confirmed, but it is still considered a key prognostic element.[127] In the present analysis, the expression of miR-146a-5p was higher in ulcerated CMs with respect to those with no ulceration ($p=0.004$) and in CMs with mitotic index $\geq 1/mm^2$ ($p=0.015$). The explanation is probably related to the faster and

higher tumoral growth: indeed, it was shown that miR-146a enhances proliferation and that a CM that mostly includes cells with elevated miR-146a expression has an advantage in proliferation.[119] Regression is defined as a host reaction characterized by a lymphocytes and macrophages infiltrate, with the lack of nests of melanocytes in the atrophic epidermis and the detection of thin dermal collagen. Regression is usually observed in almost 1/3 of the excised CMs and its impact is not totally clear. Traditionally, this parameter has been considered as an adverse prognostic factor, but recently, a possible favorable role has been proposed, likely connected to an immune-mediated response of activated T lymphocytes against the tumor.[128] Ribero et al. in 2015, published a systematic review showing that the possibility to diagnose a positive SLN are significantly lower in patients with CM showing regression with respect to those without.[129] In the present study, we did not detect a statistically significant difference in miR-146a-5p expression in CMs with regression compared to CMs without regressive features, with the exception of LMM subgroup. This finding is likely related to the inflammatory state of the neoplastic micro-environment in LMMs.

The limitations of the present PhD project include the relatively small sample size, the heterogeneity of the examined groups in the different studied areas and the greater prevalence in the HNR of LMMs with a lower medium Breslow thickness compared to the other body locations. Regarding the analysis of folliculotropism, we did not use specific immunohistochemical stainings, but we applied only a quantitative and morphologic description of the involved HFs per specimen. These findings need to be confirmed in larger series and represent only preliminary results.

CONCLUSIONS

In this project the diffuse distribution of folliculotropism (≥3 HF/specimen), the presence of atypical melanocytes into the isthmus, and the perifollicular involvement were associated with CM recurrence. The dermoscopic parameter *grey circles* in LM was correlated to the depth of folliculotropism, with a higher probability of an isthmic or bulge follicular extension of neoplastic melanocytes. The

detection of *grey circles*, *light/dark brown pseudonetwork* and *light brown structureless areas* in LMM was associated with the distribution of folliculotropism (focal/diffuse). The study shows dermatoscopic parameters that may predict follicular involvement in LM and LMM. Additionally, the detection of grey circles may assist the clinician to perform a radical excision or to obtain a biopsy in the most invasive LMM area.

MiR-146a-5p expression was shown to be significantly greater in CMs with a mitotic rate ≥1/mm2 as well as in ulcerated lesions compared to those without ulceration. No difference emerged evaluating regression when considering all CM subtypes, but an higher expression was noticed in the LMM group. Moreover, miR-146a-5p expression was lower in HNR CMs with Breslow thickness ≥0.8 mm. These results give further insights for the management of CMs with specific adverse prognostic elements. As the majority of HNR CMs are wild type of *BRAF* and *NRAS* mutations and not suitable for targeted therapies, the discovery of new molecular targets may provide relevant opportunities for the treatment.[15] Multicentric studies should be proposed to validate these findings in larger cohorts of subjects.

REFERENCES

1. Dika, E. *et al.* Clinical histopathological features and CDKN2A/CDK4/MITF mutational status of patients with multiple primary melanomas from Bologna: Italy is a fascinating but complex mosaic. *G Ital Dermatol Venereol* (2020) doi:10.23736/S0392-0488.20.06496-2.
2. Gershenwald, J. E. & Scolyer, R. A. Melanoma Staging: American Joint Committee on Cancer (AJCC) 8th Edition and Beyond. *Ann Surg Oncol* **25**, 2105–2110 (2018).
3. Broseghini, E., Dika, E., Londin, E. & Ferracin, M. MicroRNA Isoforms Contribution to Melanoma Pathogenesis. *ncRNA* **7**, 63 (2021).
4. Bruno, W. *et al.* Multiple primary melanomas (MPMs) and criteria for genetic assessment: MultiMEL, a multicenter study of the Italian Melanoma Intergroup. *Journal of the American Academy of Dermatology* **74**, 325–332 (2016).
5. Di Lorenzo, S. *et al.* Absence of germline CDKN2A mutation in Sicilian patients with familial malignant melanoma: Could it be a population-specific genetic signature? *Cancer Biol. Ther.* **17**, 83–90 (2016).
6. Leachman, S. A. *et al.* Identification, genetic testing, and management of hereditary melanoma. *Cancer and Metastasis Reviews* **36**, 77–90 (2017).
7. Dika, E., Patrizi, A., Veronesi, G., Manuelpillai, N. & Lambertini, M. Malignant cutaneous tumors of the scalp: always remember to examine the head. *J Eur Acad Dermatol Venereol* (2020) doi:10.1111/jdv.16330.

8. Soares, C. D. *et al.* Expression of mitochondrial dynamics markers during melanoma progression: Comparative study of head and neck cutaneous and mucosal melanomas. *Journal of Oral Pathology & Medicine* (2019) doi:10.1111/jop.12855.
9. Connolly, K. L., Nehal, K. S. & Lee, E. H. Quality of Life Following Surgical Excision of Early-Stage Melanoma of the Head and Neck—Reply. *JAMA Dermatology* **155**, 502 (2019).
10. Ghiasvand, R. *et al.* Association of Phenotypic Characteristics and UV Radiation Exposure With Risk of Melanoma on Different Body Sites. *JAMA Dermatology* **155**, 39 (2019).
11. Namin, A. W., Cornell, G. E., Thombs, L. A. & Zitsch, R. P. Patterns of recurrence and retreatment outcomes among clinical stage I and II head and neck melanoma patients. *Head & Neck* **41**, 1304–1311 (2019).
12. Benati, E. *et al.* Baldness and scalp melanoma. *Journal of the European Academy of Dermatology and Venereology* **31**, e528–e530 (2017).
13. Licata, G. *et al.* Diagnosis and Management of Melanoma of the Scalp: A Review of the Literature. *CCID* **Volume 14**, 1435–1447 (2021).
14. de Giorgi, V. *et al.* The prognostic impact of the anatomical sites in the 'head and neck melanoma': scalp versus face and neck. *Melanoma Res.* **22**, 402–405 (2012).
15. Dika, E. *et al.* Frequency of somatic mutations in head and neck melanoma: A single institution experience. *Pigment Cell & Melanoma Research* (2020) doi:10.1111/pcmr.12864.
16. Pereira, A. R. *et al.* Melanomas of the scalp: is hair coverage preventing early diagnosis? *Int J Dermatol* **60**, 340–346 (2021).
17. Lachiewicz, A. M., Berwick, M., Wiggins, C. L. & Thomas, N. E. Survival Differences Between Patients With Scalp or Neck Melanoma and Those With Melanoma of Other Sites in the Surveillance, Epidemiology, and End Results (SEER) Program. *Arch Dermatol* **144**, (2008).
18. Benmeir, P. *et al.* Melanoma of the Scalp: The Invisible Killer. *Plastic and Reconstructive Surgery* **95**, 496–500 (1995).
19. Elshot, Y. S. *et al.* A cohort analysis of surgically treated primary head and neck lentigo maligna (melanoma): Prognostic value of melanoma subtype and new insights in the clinical value of guideline adherence. *European Journal of Surgical Oncology* S0748798322006199 (2022) doi:10.1016/j.ejso.2022.08.012.
20. Xie, C. *et al.* Scalp melanoma: Distinctive high risk clinical and histological features. *Australasian Journal of Dermatology* **58**, 181–188 (2017).
21. Howard, M. D. *et al.* Anatomic location of primary melanoma: Survival differences and sun exposure. *Journal of the American Academy of Dermatology* **81**, 500–509 (2019).
22. Green, A. A theory of site distribution of melanomas: Queensland, Australia. *Cancer Causes Control* **3**, 513–516 (1992).
23. Abdel-Malek, Z. A., Swope, V. B., Nordlund, J. J. & Medrano, E. E. Proliferation and propagation of human melanocytes in vitro are affected by donor age and anatomical site. *Pigment Cell Res.* **7**, 116–122 (1994).
24. Millán-Esteban, D. *et al.* Mutational Characterization of Cutaneous Melanoma Supports Divergent Pathways Model for Melanoma Development. *Cancers* **13**, 5219 (2021).
25. Helsing, P. *et al.* Cutaneous head and neck melanoma (CHNM): A population-based study of the prognostic impact of tumor location. *Journal of the American Academy of Dermatology* **75**, 975-982.e2 (2016).
26. Dabouz, F. *et al.* Clinical and histological features of head and neck melanoma: a population-based study in France. *British Journal of Dermatology* **172**, 707–715 (2015).
27. Brancaccio, G. *et al.* Clark level could be still a useful prognostic marker in scalp melanoma: a multicentric cross-sectional study. *Acad Dermatol Venereol* jdv.18372 (2022) doi:10.1111/jdv.18372.
28. Lovasik, B. P. *et al.* Invasive Scalp Melanoma: Role for Enhanced Detection Through Professional Training. *Ann Surg Oncol* **23**, 4049–4057 (2016).
29. Roosta, N., Black, D. S., Wong, M. K. & Woodley, D. T. Assessing hairdressers' knowledge

of scalp and neck melanoma and their willingness to detect lesions and make referrals to dermatologists. *J Am Acad Dermatol* **68**, 183–185 (2013).
30. Shin, T. M. *et al.* Clinical and pathologic factors associated with subclinical spread of invasive melanoma. *Journal of the American Academy of Dermatology* **76**, 714–721 (2017).
31. Connolly, K. L. *et al.* Locally Recurrent Lentigo Maligna and Lentigo Maligna Melanoma: Characteristics and Time to Recurrence After Surgery. *Dermatologic Surgery* **43**, 792–797 (2017).
32. Dika, E. *et al.* Braf-V600e immunohistochemical analyses in a series of 15, Caucasian patients affected by lentigo maligna. *Acta Histochemica* **121**, 380–381 (2019).
33. Guitera, P. *et al.* A practical guide on the use of imiquimod cream to treat lentigo maligna. *Aust J Dermatology* **62**, 478–485 (2021).
34. Paus, R. & Cotsarelis, G. The Biology of Hair Follicles. *New England Journal of Medicine* **341**, 491–497 (1999).
35. Oshima, H., Rochat, A., Kedzia, C., Kobayashi, K. & Barrandon, Y. Morphogenesis and Renewal of Hair Follicles from Adult Multipotent Stem Cells. *Cell* **104**, 233–245 (2001).
36. Lyle, S. *et al.* Human Hair Follicle Bulge Cells are Biochemically Distinct and Possess an Epithelial Stem Cell Phenotype. *Journal of Investigative Dermatology Symposium Proceedings* **4**, 296–301 (1999).
37. Lyle, S. *et al.* The C8/144B monoclonal antibody recognizes cytokeratin 15 and defines the location of human hair follicle stem cells. *J Cell Sci* **111 (Pt 21)**, 3179–3188 (1998).
38. Ito, M. *et al.* Stem cells in the hair follicle bulge contribute to wound repair but not to homeostasis of the epidermis. *Nature Medicine* **11**, 1351–1354 (2005).
39. Chuong, C.-M., Jung, H.-S., Noden, D. & Widelitz, R. B. Lineage and pluripotentiality of epithelial precursor cells in developing chicken skin. *Biochemistry and Cell Biology* **76**, 1069–1077 (1998).
40. Danilenko, D. M., Ring, B. D. & Pierce, G. F. Growth factors and cytokines in hair follicle development and cycling: recent insights from animal models and the potentials for clinical therapy. *Molecular Medicine Today* **2**, 460–467 (1996).
41. Tiede, S. *et al.* Hair follicle stem cells: Walking the maze. *European Journal of Cell Biology* **86**, 355–376 (2007).
42. Nishimura, E. K. Mechanisms of Hair Graying: Incomplete Melanocyte Stem Cell Maintenance in the Niche. *Science* **307**, 720–724 (2005).
43. Nishimura, E. K. *et al.* Dominant role of the niche in melanocyte stem-cell fate determination. *Nature* **416**, 854–860 (2002).
44. Lako, M. Hair follicle dermal cells repopulate the mouse haematopoietic system. *Journal of Cell Science* **115**, 3967–3974 (2002).
45. Yu, H. *et al.* Isolation of a Novel Population of Multipotent Adult Stem Cells from Human Hair Follicles. *The American Journal of Pathology* **168**, 1879–1888 (2006).
46. Cook, M. G., Spatz, A., Bröcker, E.-B. & Ruiter, D. J. Identification of histological features associated with metastatic potential in thin (<1.0 mm) cutaneous melanoma with metastases. A study on behalf of the EORTC Melanoma Group: Histological features associated with metastatic potential in thin (<1.0 mm) cutaneous melanoma with metastases. *The Journal of Pathology* **197**, 188–193 (2002).
47. Hantschke, M., Mentzel, T. & Kutzner, H. Follicular malignant melanoma: a variant of melanoma to be distinguished from lentigo maligna melanoma. *Am J Dermatopathol* **26**, 359–363 (2004).
48. Pozdnyakova, O., Grossman, J., Barbagallo, B. & Lyle, S. The hair follicle barrier to involvement by malignant melanoma. *Cancer* **115**, 1267–1275 (2009).
49. Cotsarelis, G. Epithelial Stem Cells: A Folliculocentric View. *Journal of Investigative Dermatology* **126**, 1459–1468 (2006).
50. Ohyama, M. Characterization and isolation of stem cell-enriched human hair follicle bulge cells. *Journal of Clinical Investigation* **116**, 249–260 (2005).

51. Ilmonen, S., Jahkola, T., Turunen, J. P., Muhonen, T. & Asko-Seljavaara, S. Tenascin-C in primary malignant melanoma of the skin. *Histopathology* **45**, 405–411 (2004).
52. Markowicz, S. *et al.* Anticancer Properties of Peptide Fragments of Hair Proteins. *PLoS ONE* **9**, e98073 (2014).
53. Scolyer, R. A. *et al.* Data Set for Pathology Reporting of Cutaneous Invasive Melanoma: Recommendations From the International Collaboration on Cancer Reporting (ICCR). *The American Journal of Surgical Pathology* **37**, 1797–1814 (2013).
54. Tjarks, B. J., Somani, N., Piliang, M. & Bergfeld, W. F. A proposed classification for follicular involvement by melanoma: Patterns of follicular involvement by melanoma. *Journal of Cutaneous Pathology* **44**, 45–52 (2017).
55. Breslow, A. Thickness, cross-sectional areas and depth of invasion in the prognosis of cutaneous melanoma. *Ann. Surg.* **172**, 902–908 (1970).
56. Djebali, S. *et al.* Landscape of transcription in human cells. *Nature* **489**, 101–108 (2012).
57. Moraes, F. & Góes, A. A decade of human genome project conclusion: Scientific diffusion about our genome knowledge: A Decade of Human Genome Project Conclusion. *Biochem. Mol. Biol. Educ.* **44**, 215–223 (2016).
58. Riefolo, M., Porcellini, E., Dika, E., Broseghini, E. & Ferracin, M. Interplay between small and long non-coding RNAs in cutaneous melanoma: a complex jigsaw puzzle with missing pieces. *Molecular Oncology* **13**, 74–98 (2019).
59. Dika, E. *et al.* Defining the prognostic role of microRNAs in cutaneous melanoma. *J. Invest. Dermatol.* (2020) doi:10.1016/j.jid.2020.03.949.
60. Xu, Y., Brenn, T., Brown, E. R. S., Doherty, V. & Melton, D. W. Differential expression of microRNAs during melanoma progression: miR-200c, miR-205 and miR-211 are downregulated in melanoma and act as tumour suppressors. *British Journal of Cancer* **106**, 553–561 (2012).
61. Levy, C. *et al.* Intronic miR-211 Assumes the Tumor Suppressive Function of Its Host Gene in Melanoma. *Molecular Cell* **40**, 841–849 (2010).
62. Mazar, J. *et al.* The Regulation of miRNA-211 Expression and Its Role in Melanoma Cell Invasiveness. *PLoS ONE* **5**, e13779 (2010).
63. Hammock, L. *et al.* Chromogenic in situ hybridization analysis of melastatin mRNA expression in melanomas from American Joint Committee on Cancer stage I and II patients with recurrent melanoma. *Journal of Cutaneous Pathology* **33**, 599–607 (2006).
64. Ren, J.-W., Li, Z.-J. & Tu, C. MiR-135 post-transcriptionally regulates FOXO1 expression and promotes cell proliferation in human malignant melanoma cells. *Int J Clin Exp Pathol* **8**, 6356–6366 (2015).
65. Grignol, V. *et al.* miR-21 and miR-155 are associated with mitotic activity and lesion depth of borderline melanocytic lesions. *British Journal of Cancer* **105**, 1023–1029 (2011).
66. Jiang, L. *et al.* The status of microRNA-21 expression and its clinical significance in human cutaneous malignant melanoma. *Acta Histochemica* **114**, 582–588 (2012).
67. Schultz, J., Lorenz, P., Gross, G., Ibrahim, S. & Kunz, M. MicroRNA let-7b targets important cell cycle molecules in malignant melanoma cells and interferes with anchorage-independent growth. *Cell Research* **18**, 549–557 (2008).
68. Wu, J., Li, J., Ren, J. & Zhang, D. MicroRNA-485-5p represses melanoma cell invasion and proliferation by suppressing Frizzled7. *Biomedicine & Pharmacotherapy* **90**, 303–310 (2017).
69. Wang, S. *et al.* Characterization of long noncoding RNA and messenger RNA signatures in melanoma tumorigenesis and metastasis. *PLOS ONE* **12**, e0172498 (2017).
70. Zhu, Y., Wen, X. & Zhao, P. MicroRNA-365 Inhibits Cell Growth and Promotes Apoptosis in Melanoma by Targeting BCL2 and Cyclin D1 (CCND1). *Medical Science Monitor* **24**, 3679–3692 (2018).
71. Georgantas, R. W. *et al.* MicroRNA-206 induces G1 arrest in melanoma by inhibition of CDK4 and Cyclin D. *Pigment Cell & Melanoma Research* **27**, 275–286 (2014).
72. Holst, L. M. B. *et al.* The microRNA molecular signature of atypic and common acquired

melanocytic nevi: differential expression of miR-125b and let-7c: Letter to the Editor. *Experimental Dermatology* **20**, 278–280 (2011).
73. Komina, A., Palkina, N., Aksenenko, M., Tsyrenzhapova, S. & Ruksha, T. Antiproliferative and Pro-Apoptotic Effects of MiR-4286 Inhibition in Melanoma Cells. *PLOS ONE* **11**, e0168229 (2016).
74. Nyholm, A. M. *et al.* miR-125b induces cellular senescence in malignant melanoma. *BMC Dermatology* **14**, (2014).
75. Dar, A. A. *et al.* miRNA-205 Suppresses Melanoma Cell Proliferation and Induces Senescence via Regulation of E2F1 Protein. *Journal of Biological Chemistry* **286**, 16606–16614 (2011).
76. Reuland, S. N. *et al.* MicroRNA-26a Is Strongly Downregulated in Melanoma and Induces Cell Death through Repression of Silencer of Death Domains (SODD). *Journal of Investigative Dermatology* **133**, 1286–1293 (2013).
77. Segura, M. F. *et al.* Melanoma MicroRNA Signature Predicts Post-Recurrence Survival. *Clinical Cancer Research* **16**, 1577–1586 (2010).
78. Fleming, N. H. *et al.* Serum-based miRNAs in the prediction and detection of recurrence in melanoma patients: Prognostic Serum miRNAs in Melanoma. *Cancer* **121**, 51–59 (2015).
79. Howard, J. D. *et al.* Notch signaling mediates melanoma-endothelial cell communication and melanoma cell migration. *Pigment Cell & Melanoma Research* **26**, 697–707 (2013).
80. Kunz, M. MicroRNAs in Melanoma Biology. in *MicroRNA Cancer Regulation* (eds. Schmitz, U., Wolkenhauer, O. & Vera, J.) vol. 774 103–120 (Springer Netherlands, 2013).
81. Walker, M. J., Silliman, E., Dayton, M. A. & Lang, J. C. The expression of C-myb in human metastatic melanoma cell lines and specimens. *Anticancer Res* **18**, 1129–1135 (1998).
82. Boyle, G. M. *et al.* Melanoma cell invasiveness is regulated by miR-211 suppression of the BRN2 transcription factor: miR-211 regulates melanoma invasiveness via BRN2. *Pigment Cell & Melanoma Research* **24**, 525–537 (2011).
83. Elson-Schwab, I., Lorentzen, A. & Marshall, C. J. MicroRNA-200 Family Members Differentially Regulate Morphological Plasticity and Mode of Melanoma Cell Invasion. *PLoS ONE* **5**, e13176 (2010).
84. Segura, M. F. *et al.* Aberrant miR-182 expression promotes melanoma metastasis by repressing FOXO3 and microphthalmia-associated transcription factor. *Proceedings of the National Academy of Sciences* **106**, 1814–1819 (2009).
85. Martin del Campo, S. E. *et al.* MiR-21 Enhances Melanoma Invasiveness via Inhibition of Tissue Inhibitor of Metalloproteinases 3 Expression: In Vivo Effects of MiR-21 Inhibitor. *PLOS ONE* **10**, e0115919 (2015).
86. Yang, C. H., Yue, J., Pfeffer, S. R., Handorf, C. R. & Pfeffer, L. M. MicroRNA miR-21 Regulates the Metastatic Behavior of B16 Melanoma Cells. *Journal of Biological Chemistry* **286**, 39172–39178 (2011).
87. Liu, S. *et al.* MicroRNA-9 up-regulates E-cadherin through inhibition of NF-κB1-Snail1 pathway in melanoma: miR-9 inhibits melanoma progression. *The Journal of Pathology* **226**, 61–72 (2012).
88. Chang, X. *et al.* miR-203 inhibits melanoma invasive and proliferative abilities by targeting the polycomb group gene BMI1. *Biochemical and Biophysical Research Communications* **456**, 361–366 (2015).
89. Kappelmann, M., Kuphal, S., Meister, G., Vardimon, L. & Bosserhoff, A.-K. MicroRNA miR-125b controls melanoma progression by direct regulation of c-Jun protein expression. *Oncogene* **32**, 2984–2991 (2013).
90. Zhang, D., Han, Y. & Xu, L. RETRACTED: Upregulation of miR-124 by physcion 8-O-β-glucopyranoside inhibits proliferation and invasion of malignant melanoma cells via repressing RLIP76. *Biomedicine & Pharmacotherapy* **84**, 166–176 (2016).
91. Zeng, H. F., Yan, S. & Wu, S. F. MicroRNA-153-3p suppress cell proliferation and invasion

by targeting SNAI1 in melanoma. *Biochemical and Biophysical Research Communications* **487**, 140–145 (2017).
92. Liu, R. *et al.* Identification of FLOT2 as a novel target for microRNA-34a in melanoma. *Journal of Cancer Research and Clinical Oncology* **141**, 993–1006 (2015).
93. Giles, K. M. *et al.* microRNA-7-5p inhibits melanoma cell proliferation and metastasis by suppressing RelA/NF-κB. *Oncotarget* **7**, 31663–31680 (2016).
94. El Sharouni, M.-A., Witkamp, A. J., Sigurdsson, V. & van Diest, P. J. Comparison of Survival Between Patients With Single vs Multiple Primary Cutaneous Melanomas. *JAMA Dermatol* **155**, 1049 (2019).
95. Doubrovsky, A. & Menzies, S. W. Enhanced Survival in Patients With Multiple Primary Melanoma. *Arch Dermatol* **139**, (2003).
96. Dika, E. *et al.* Unraveling the role of microRNA/isomiR network in multiple primary melanoma pathogenesis. *Cell Death Dis* **12**, 473 (2021).
97. Cloonan, N. *et al.* MicroRNAs and their isomiRs function cooperatively to target common biological pathways. *Genome Biol* **12**, R126 (2011).
98. Kim, V. N. MicroRNA biogenesis: coordinated cropping and dicing. *Nat Rev Mol Cell Biol* **6**, 376–385 (2005).
99. Bhoyrul, B. *et al.* Pathological review of primary cutaneous malignant melanoma by a specialist skin cancer multidisciplinary team improves patient care in the UK. *J Clin Pathol* **72**, 482–486 (2019).
100. Schmittgen, T. D. & Livak, K. J. Analyzing real-time PCR data by the comparative CT method. *Nat Protoc* **3**, 1101–1108 (2008).
101. Tiodorovic-Zivkovic, D. *et al.* The importance of gray color as a dermoscopic clue in facial pigmented lesion evaluation: a case report. *Dermatology Practical & Conceptual* **3**, (2013).
102. Schiffner, R. *et al.* Improvement of early recognition of lentigo maligna using dermatoscopy. *Journal of the American Academy of Dermatology* **42**, 25–32 (2000).
103. Tanaka, M., Sawada, M. & Kobayashi, K. Key points in dermoscopic differentiation between lentigo maligna and solar lentigo: Dermoscopy of lentigo maligna. *The Journal of Dermatology* **38**, 53–58 (2011).
104. Zalaudek, I. *et al.* Problematic Lesions in the Elderly. *Dermatologic Clinics* **31**, 549–564 (2013).
105. Annessi, G., Bono, R. & Abeni, D. Correlation between digital epiluminescence microscopy parameters and histopathological changes in lentigo maligna and solar lentigo: A dermoscopic index for the diagnosis of lentigo maligna. *Journal of the American Academy of Dermatology* **76**, 234–243 (2017).
106. Cinotti, E. *et al.* The integration of dermoscopy and reflectance confocal microscopy improves the diagnosis of lentigo maligna. *J Eur Acad Dermatol Venereol* **33**, (2019).
107. de Carvalho, N. *et al.* Reflectance confocal microscopy correlates of dermoscopic patterns of facial lesions help to discriminate lentigo maligna from pigmented nonmelanocytic macules. *Br J Dermatol* **173**, 128–133 (2015).
108. Nascimento, M. M. *et al.* Inner gray halo, a novel dermoscopic feature for the diagnosis of pigmented actinic keratosis: Clues for the differential diagnosis with lentigo maligna. *Journal of the American Academy of Dermatology* **71**, 708–715 (2014).
109. Zalaudek, I. *et al.* Three Roots of Melanoma. *Arch Dermatol* **144**, (2008).
110. Schweizer, A. *et al.* Differentiation of combined nevi and melanomas: Case-control study with comparative analysis of dermoscopic features. *JDDG: Journal der Deutschen Dermatologischen Gesellschaft* **18**, 111–118 (2020).
111. Zalaudek, I. *et al.* Flat pigmented macules on sun-damaged skin of the head/neck: Junctional nevus, atypical lentiginous nevus, or melanoma in situ? *Clinics in Dermatology* **32**, 88–93 (2014).
112. Connolly, K. L., Nijhawan, R. I., Dusza, S. W., Busam, K. J. & Nehal, K. S. Time to local recurrence of lentigo maligna: Implications for future studies. *Journal of the American Academy of*

Dermatology **74**, 1247–1248 (2016).
113. Tschandl, P., Rosendahl, C. & Kittler, H. Dermatoscopy of flat pigmented facial lesions. *J Eur Acad Dermatol Venereol* **29**, 120–127 (2015).
114. Shain, A. H. *et al.* The Genetic Evolution of Melanoma from Precursor Lesions. *N Engl J Med* **373**, 1926–1936 (2015).
115. Sellheyer, K. Pathogenesis of solar elastosis: synthesis or degradation?: **Solar elastosis**. *Journal of Cutaneous Pathology* **30**, 123–127 (2003).
116. Tate, J. G. *et al.* COSMIC: the Catalogue Of Somatic Mutations In Cancer. *Nucleic Acids Research* **47**, D941–D947 (2019).
117. Forloni, M. *et al.* miR-146a promotes the initiation and progression of melanoma by activating Notch signaling. *eLife* **3**, e01460 (2014).
118. Aksenenko, M., Palkina, N., Komina, A., Tashireva, L. & Ruksha, T. Differences in microRNA expression between melanoma and healthy adjacent skin. *BMC Dermatol* **19**, 1 (2019).
119. Raimo, M. *et al.* miR-146a Exerts Differential Effects on Melanoma Growth and Metastatization. *Mol Cancer Res* **14**, 548–562 (2016).
120. Pu, W., Shang, Y., Shao, Q. & Yuan, X. miR-146a promotes cell migration and invasion in melanoma by directly targeting SMAD4. *Oncol Lett* (2018) doi:10.3892/ol.2018.8172.
121. Awad, F. *et al.* Photoaging and skin cancer: Is the inflammasome the missing link? *Mechanisms of Ageing and Development* **172**, 131–137 (2018).
122. Hodis, E. *et al.* A Landscape of Driver Mutations in Melanoma. *Cell* **150**, 251–263 (2012).
123. Sha, J. *et al.* The Response of microRNAs to Solar UVR in Skin-Resident Melanocytes Differs between Melanoma Patients and Healthy Persons. *PLoS ONE* **11**, e0154915 (2016).
124. Rebane, A. & Akdis, C. A. MicroRNAs: Essential players in the regulation of inflammation. *Journal of Allergy and Clinical Immunology* **132**, 15–26 (2013).
125. Curtale, G. *et al.* An emerging player in the adaptive immune response: microRNA-146a is a modulator of IL-2 expression and activation-induced cell death in T lymphocytes. *Blood* **115**, 265–273 (2010).
126. Perry, M. M., Williams, A. E., Tsitsiou, E., Larner-Svensson, H. M. & Lindsay, M. A. Divergent intracellular pathways regulate interleukin-1β-induced miR-146a and miR-146b expression and chemokine release in human alveolar epithelial cells. *FEBS Letters* **583**, 3349–3355 (2009).
127. Gershenwald, J. E. *et al.* Melanoma staging: Evidence-based changes in the American Joint Committee on Cancer eighth edition cancer staging manual. *CA Cancer J Clin* **67**, 472–492 (2017).
128. Ribero, S. Histological regression in primary melanoma and drug-related immune reaction towards metastatic melanoma: Are they associated?? *Medical Hypotheses* **143**, 110019 (2020).
129. Ribero, S. *et al.* Association of Histologic Regression in Primary Melanoma With Sentinel Lymph Node Status: A Systematic Review and Meta-analysis. *JAMA Dermatol* **151**, 1301 (2015).